(5) P. J. Crowley and H. M. Haendler, *Inorg. Chem.*, **1**, 904 (1962).
(6) J. A. McCleverty, *Prog. Inorg. Chem.*, **10**, 49 (1968).
(7) Y. S. Sohn and A. L. Balch, *J. Am. Chem. Soc.*, **93**, 1290 (1971).
(8) A. L. Balch and Y. S. Sohn, *J. Organomet. Chem.*, **30**, C31 (1971).
(9) A. L. Balch, *J. Am. Chem. Soc.*, **95**, 2723 (1973).
(10) J. E. Dickeson and L. A. Summers, *Aust. J. Chem.*, **23**, 1023 (1970).
(11) L. F. Fieser, "Organic Syntheses", Collect. Vol. 2, Wiley, New York, N.Y., 1943, pp 35, 430.
(12) J. Schmidt and E. Junghans, *Ber. Dtsch. Chem. Ges.*, **37**, 3558 (1904).
(13) J. J. Levison and S. D. Robinson, *J. Chem. Soc. A*, 2947 (1970).
(14) T. A. Stephenson and G. Wilkinson, *J. Inorg. Nucl. Chem.*, **28**, 945 (1966).
(15) L. Malatesta and M. Angoletta, *J. Chem. Soc.*, 1186 (1957).
(16) M. J. Cleare and W. P. Griffith, *J. Chem. Soc. A*, 2788 (1970).
(17) A. Davison, N. Edelstein, R. H. Holm, and A. H. Maki, *Inorg. Chem.*, **2**, 1227 (1963).
(18) A. Earnshaw, B. N. Figgis, J. Lewis, and R. D. Peacock, *J. Chem. Soc.*, 3132 (1961).
(19) S. Cenini, R. Ugo, and G. La Monica, *J. Chem. Soc. A*, 416 (1971).
(20) R. D. Gillard, R. E. E. Hill, and R. Maskill, *J. Chem. Soc. A*, 1447 (1970).
(21) R. S. Nicholson and I. Shain, *Anal. Chem.*, **36**, 706 (1964).
(22) J. E. Wertz and J. L. Vivo, *J. Chem. Phys.*, **23**, 2441 (1955).
(23) A. Hudson and M. J. Kenney, *J. Chem. Soc. A*, 1116 (1969).

Contribution from the School of Chemical Sciences, University of Illinois, Urbana, Illinois 61801

Electron Transfer in Oxidized Biferrocene, Biferrocenylene, and [1.1]Ferrocenophane Systems

WILLIAM H. MORRISON, Jr. and DAVID N. HENDRICKSON*[1]

Received January 3, 1975 AIC500148

Oxidized salts of biferrocene, 1',6'-diiodobiferrocene, biferrocenylene, and 1,12-dimethyl[1.1]ferrocenophane are studied with ^{57}Fe Mössbauer spectroscopy, variable-temperature magnetic susceptibility, and X-band EPR, infrared, and electronic absorption spectroscopies with the objective of determining the "intervalence" electron-transfer rates in the singly oxidized species and relating the rates to the level of exchange-type interaction present. The compound biferricenium$^+$TCA$^-$·2TCAA shows ^{57}Fe Mössbauer spectra at 300 and 4.2°K that are interpretable in terms of a superposition of two quadrupole-split doublets (ΔE_Q = 2.176 and 0.392 mm/sec at 300°K) for a mixed-valence $Fe^{II}Fe^{III}$ species and one lower intensity doublet (ΔE_Q = 0.903 mm/sec at 300°K) for an average-valence species. It is speculated that the flexibility of the singly fused, singly oxidized biferrocene ion appears to lead to some anion dependence in the electron-transfer rate. Singly oxidized 1',6'-diiodobiferrocene is a delocalized system (i.e., average valence) as characterized by Mössbauer spectroscopy (one doublet with ΔE_Q = 1.284 mm/sec at 300°K) and EPR (g_1 = 2.75, g_2 = 2.01, and g_3 = 1.97 for the solid at 12°K). A relatively isotropic g tensor ($g_1 \simeq 2.3$, $g_2 \simeq 2.0$, and $g_3 \simeq 1.9$) is also seen for the delocalized singly oxidized biferrocenylene ion in four salts and it is shown that for these fused ferrocene–ferricenium systems the conversion from mixed valence to average valence is characterized by a loss of orbital angular momentum (giving a relatively isotropic g tensor) as a result of the delocalization of the single unpaired electron onto two iron centers. The absence of the usual ferricenium $^2E_{1u} \leftarrow {}^2E_{2g}$ "hole" transition is explained for diamagnetic biferricenylenium(2+). The infrared spectra of biferrocenylene and biferricenylenium(n+) (n = 1, 2) are discussed. The unusual temperature dependence of the Mössbauer spectrum of 1,12-dimethyl[1.1]ferricenophanium$^+I_3^-$ is reinvestigated and data are presented for measurements at 300, 190, 140, 100, 80, and 4.2°K. It is suggested that the inner doublet for the Fe(III) site is tending to convert to a magnetic spectrum at the lowest temperatures. Finally and most importantly, evidence is presented to support the presence of direct Fe–Fe interaction in these systems by the reporting of *diamagnetism* for the DDQH$^-$ salt of dioxidized [$Fe^{III}Fe^{III}$] 1,12-dimethyl[1.1]-ferrocenophane. A 4.2°K magnetically perturbed Mössbauer spectrum, which shows $\eta = \sim 0.8$, is also presented for this same compound.

Introduction

The increased interest in mixed-valence compounds in recent years stems from attempts to make high-temperature superconducting materials and new semiconducting materials, increased interest in understanding biological mixed-valence compounds (most notably the ferredoxin systems), analogies between mixed-valence compounds and inner- and outer-sphere complexes formed during redox processes, and simply a renewed curiosity as to the intriguing characteristics of mixed-valence and analogous average-valence (i.e., delocalized) systems. The last is perhaps tempered by a feeling that an understanding of the mixed-valence phenomenon will in itself lead to a better understanding of the electronic structure of simpler systems. Results from a few concerted and continuing programs have appeared since the 1967 reviews[2-4] on mixed-valence compounds. Germane to this paper is the work[5-20] on mixed-valence biferrocene-type compounds; mixed-valence ferrocene polymers have also been reported.[21-24]

In this paper results will be reported on new biferricenium salts such as the trichloroacetate salt (TCA$^-$ stands for trichloroacetate and TCAA for trichloroacetic acid) of monooxidized biferrocene (I, n = 1) and the I_3^- salt of monooxidized 1',6'-diiodobiferrocene (II, n = 1), and results will be presented for various biferrocenylene(III) and [1.1]ferrocenophane(IV) systems, most notably the magnetism and ^{57}Fe Mössbauer results for the 2,3-dichloro-5,6-dicyanobenzoquinone salt of dioxidized 1,12-dimethyl[1.1]ferrocenophane (IVb, n = 2).

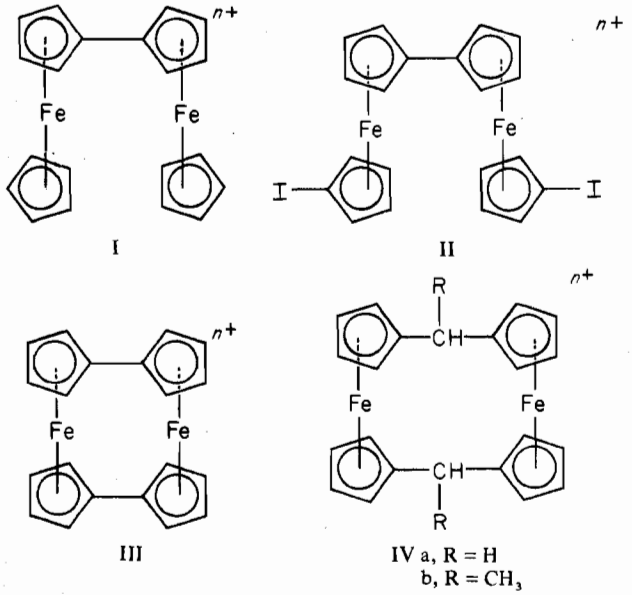

Cowan and Kaufman[5] first prepared a salt of monooxidized biferrocene (I, n = 1) and reported that the cation was of the mixed-valence type, i.e., possessed both a low-spin Fe(II) and

a low-spin Fe(III) center, or, more explicity, the intervalence transfer rate was less than the ^{57}Fe Mössbauer time scale (rate $< 10^7$ sec^{-1}). It has since been found that monooxidized biferrocenylene (III, $n = 1$) is of the average-valence type (that is, the odd electron is delocalized in a molecular orbital encompassing both iron centers), and it has been reported that the monooxidized [1.1]ferrocenophanes (IVa and IVb with $n = 1$) have electron transfer rates slower than $\sim 10^7$ sec^{-1} at 300°K. The transition from mixed-valence to average-valence type is reflected in the various physical properties (e.g., magnetic susceptibility, EPR, and ^{57}Fe Mössbauer) of a given system and in this paper we will explain and delineate the types of changes that occur. The viability of electron transfer by either direct exchange via an Fe–Fe interaction or superexchange via the ring moieties for the above molecules will be discussed.

Results and Discussion

Biferrocene Systems. Cowan et al.[5-12] have reported the results of various studies of the mixed-valence system biferricenium picrate, i.e., the picrate of cation I, $n = 1$. In solution they found that the thermal electron transfer in the cation was faster than the NMR time scale, k(thermal) $> 10^6$ sec^{-1}. The biferricenium cation in solution also exhibits, in the near-infrared region, an intervalence-transfer (IT) electronic absorption band and from this Cowan calculated k(thermal) $= 1.3 \times 10^{10}$ sec^{-1} using the theoretical expressions of Hush.[4] Diffuse electronic reflectance spectra of the solid also gave the same estimate of k(thermal). However, ^{57}Fe Mössbauer experiments at 77°K on the solid clearly showed that in respect to the ^{57}Fe Mössbauer time scale (^{57}Fe nuclear excited-state lifetime of $\sim 10^{-7}$ sec) there are two different iron atoms in the cation, one a low-spin Fe(II) and the other a low-spin Fe(III). Weak shoulders not present at 77°K and perhaps indicative of an average-valence species were noted in the room-temperature spectrum. It was suggested by Cowan that this might indicate that the thermal intervalence transfer rate is on the order of 10^7 sec^{-1}.

It did seem to us at the time of their reporting and with our latter work[17] that the Mössbauer observations and interpretation were the most straightforward and that an erroneous determination of k(thermal) is obtained from the IT band, a point to which we will return. The potential flexibility of cation I, $n = 1$, is evident and as such one could expect that different salts could have different properties. It was with this in mind that we prepared and studied[17] the I_3^- salt of cation I, $n = 1$. The IT band was found to be the same as reported by Cowan for the picrate. The ^{57}Fe Mössbauer spectrum of the I_3^- salt at 4.2°K showed two equal-area quadrupole-split doublets as expected for a mixed-valence compound. In contrast to Cowan's findings, however, the 300°K spectrum did *not* show an additional weak doublet. A very recent report[25] on the picrate salt also does not show the additional shoulders reported by Cowan.

To investigate further the anion effect we prepared some analytically pure (see Table I), crystalline samples of biferricenium$^+$TCA$^-$·2TCAA, that is, the trichloroacetate salt of cation I, $n = 1$. The analogous ferricenium compound, i.e., [Fe(cp)$_2$]TCA·2TCAA, is known, and, in fact, its X-ray crystal structure shows a ferricenium cation with eclipsed rings and a TCA$^-$ anion hydrogen bonded to two TCAA molecules.[26] Iron-57 Mössbauer spectra were run for biferricenium$^+$TCA$^-$·2TCAA at 300 and 4.2°K and they are reproduced in Figure 1. It is evident that upon cooling the sample from 300 to 4.2°K there is a significant change in the Mössbauer spectrum in that there is an apparent loss of intensity in the central features relative to the outside doublet. Recall that ferrocene exhibits a doublet with a relatively large quadrupole splitting, ΔE_Q, of 2.4 mm/sec and that the ferricenium ion has a small ΔE_Q in the range of 0.0–0.08 mm/sec.[27] As was the case for the triiodide salt, a mixed-valence spectrum would have two doublets and the areas of the two doublets would be equal. Attempts to fit by least squares (lorenztian line shapes) the 300°K spectrum in Figure 1 with *two* quadrupole-split doublets showed that the area of the central "doublet" is in excess of that for the outer quadrupole-split doublet. Close inspection of the 300°K spectrum points to the presence of some shoulders on the center doublet. The 300°K Mössbauer spectrum was obtained for a second sample of the trichloroacetate compound and this time a more contracted velocity range was selected for data collection. Figure 2 shows that there are shoulders on the

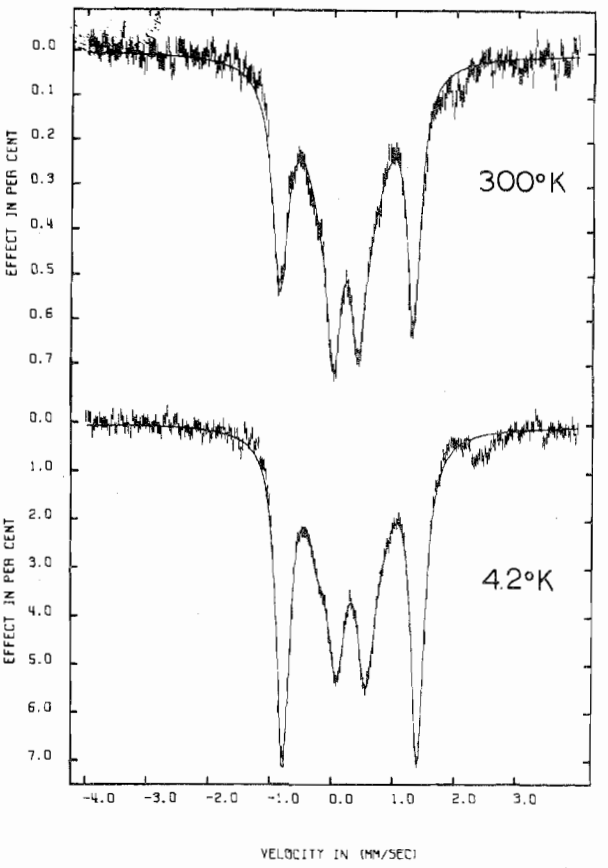

Figure 1. ^{57}Fe Mössbauer spectra for biferricenium$^+$TCA$^-$·2TCAA at 300 and 4.2°K. The velocity scale is referenced to the Co in Cu source.

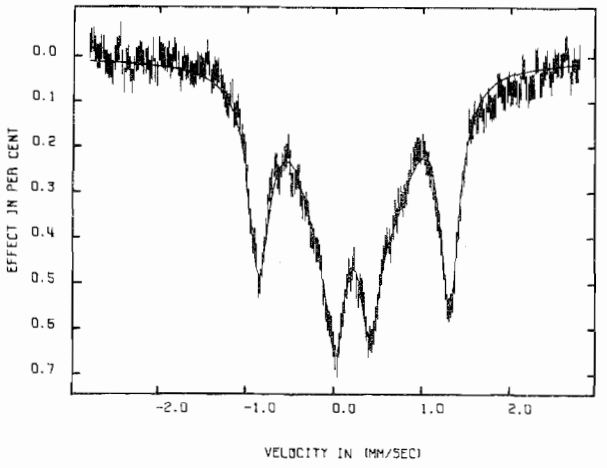

Figure 2. ^{57}Fe Mössbauer spectrum run on a more contracted velocity range for a second sample of biferricenium$^+$TCA$^-$·2TCAA at 300°K. The velocity scale is referenced to the Co in Cu source.

Table I. Analytical Data[a]

Compd	% calcd			% found		
	C	H	Fe	C	H	Fe
Biferrocene	64.91	4.90		64.73	5.18	
Biferricenium$^+I_3^-$ [b]	32.24	2.41	14.86	32.30	2.50	14.63
Biferricenium$^+$TCA$^-$·2TCAA	36.35	2.13	13.00	36.16	2.31	13.04
Biferricenium^{2+}(DDQH$^-$)$_2$	52.34	2.44	13.52	52.62	2.08	13.41
Ferricenium$^+I_3^-$ [c]	21.19	1.78	9.85	21.14	1.79	10.26
Ferricenium$^+$DDQH$^-$	52.22	2.68	13.49	52.85	2.54	13.43
1′,6′-diiodobiferricenium$^+I_3^-$	23.96	1.61	11.14	24.77	2.17	11.15
Biferrocenylene	65.27	4.38		65.12	4.18	
Biferricenylenium$^+I_2^-$	38.63	2.59	17.96	37.86	2.63	17.45
				37.63	2.38	17.35
				38.36	2.47	
Biferricenylenium$^+I_5^-$	23.96	1.61	11.14	24.07	1.62	11.07
				23.89	1.51	11.58
Biferricenylenium$^+PF_6^-$	46.83	3.14	21.77	47.11	3.16	21.70
Biferricenylenium$^+$TCA$^-$·2TCAA	36.43	2.12	13.03	34.03	1.97	11.44
Biferricenylenium^{2+}(PF$_6^-$)$_2$	36.51	2.45	16.98	36.95	2.48	17.05
Biferricenylenium^{2+}(DDQH$^-$)$_2$	52.47	2.20	13.55	53.62	2.16	13.88
1,12-Dimethyl[1.1]ferrocenophane	78.69	6.06	15.25	79.22	6.10	14.97
1,12-Dimethyl[1.1]ferricenophanium$^+I_3^-$	35.82	3.01	13.88	35.76	2.79	13.83
[1,1]ferricenophanium$^+I_3^-$·0.5I_2	29.24	2.23	12.36	28.60	2.04	12.00
1,12-Dimethyl[1.1]ferricenophanium^{2+}(DDQH$^-$)$_2$ [d]	54.58	2.98	12.69	54.23	3.03	11.78

[a] For some compounds the results of analyses of different preparations are indicated. [b] Iodine analysis: calcd, 50.73; found, 50.41. [c] Iodine analysis: calcd, 67.17; found 66.89. [d] Nitrogen analysis: calcd, 6.37; found, 6.45.

Table II. Iron-57 Mössbauer Data and Fitting Parameters for Biferrocene and Biferrocenylene Systems[a]

Compd	Temp, °K	ΔE_Q	δ[b]	Γ[c]
Biferricenium$^+I_3^-$	300	2.013 (5)	0.432 (5)	0.351 (8), 0.281 (6)
		0.400 (5)	0.435 (5)	0.313 (8), 0.320 (8)
	4.2	2.119 (3)	0.519 (3)	0.308 (4), 0.268 (4)
		0.381 (3)	0.531 (3)	0.303 (4), 0.303 (4)
Biferricenium picrate[d]	298	2.053	0.419	
		0.302	0.421	
	77	2.141	0.510	
		0.288	0.518	
Biferricenium$^+$TCA$^-$·2TCAA[e]	300	2.176 (6)	0.441 (6)	0.317 (7), 0.271 (6)
		0.903 (29)	0.450 (29)	0.597 (37), 0.597 (37)
		0.392 (7)	0.435 (7)	0.310 (6), 0.323 (6)
	4.2	2.183 (3)	0.534 (3)	0.258 (3), 0.264 (3)
		1.015 (52)	0.509 (52)	0.369 (32), 0.514 (36)
		0.474 (13)	0.542 (13)	0.376 (10), 0.372 (9)
Biferricenium^{2+}(BF$_4^-$)$_2$[d]	77	0.163	0.497	
1′,6′-Diiodobiferricenium$^+I_3^-$	300	1.284 (6)	0.428 (6)	0.257 (6), 0.244 (5)
	4.2	1.388 (2)	0.532 (2)	0.339 (2), 0.343 (2)
Biferricenylenium$^+I_5^-$	300	1.719 (3)	0.441 (3)	0.265 (4), 0.331 (6)
	4.2	1.756 (2)	0.542 (2)	0.291 (3), 0.338 (5)
Biferricenylenium$^+PF_6^-$[f]	300	1.738 (22)	0.403 (20)	0.255 (22), 0.230 (19)
	4.2	1.816 (5)	0.527 (5)	0.277 (4), 0.272 (4)
Biferricenylenium$^+$DDQH$^-$[f]	300	1.784 (13)	0.440 (13)	0.368 (12), 0.354 (12)
	4.2	1.726 (8)	0.520 (8)	0.413 (7), 0.425 (7)
Biferricenylenium picrate[g]	298	1.75	0.436	0.3, 0.3
	77	1.78	0.525	0.3, 0.3
Biferricenylenium^{2+}(PF$_6^-$)$_2$	300	2.890 (2)	0.467 (2)	0.253 (2), 0.234 (1)
	4.2	2.950 (1)	0.567 (1)	0.288 (1), 0.279 (1)
Biferricenylenium^{2+}(DDQH$^-$)$_2$	300	2.833 (4)	0.476 (4)	0.309 (4), 0.280 (4)
	4.2	2.951 (2)	0.573 (2)	0.312 (2), 0.301 (2)
Biferrocenylene	300	2.397 (1)	0.434 (1)	0.282 (2), 0.261 (2)
	80	2.398 (1)	0.508 (1)	0.388 (3), 0.378 (3)
	4.2	2.405 (1)	0.531 (1)	0.363 (2), 0.358 (2)
Biferrocene[h]	78	2.36	0.52	

[a] ΔE_Q, δ, and Γ values are in mm/sec; estimated significant figures from least-squares fitting to lorentzian peaks are given in parentheses. [b] Isomer shift relative to iron foil. [c] Full width at half-height taken from the lorentzian fitting program. The line at the more negative velocity is listed first. [d] See ref 7. [e] At room temperature the "average-valence" site has an area via the fitting that is 76% of either of the other two equal-area doublets; at 4.2°K it was only 31% of the area of either of the two equal-area doublets. [f] These parameters were obtained by fitting the signal from the small amount (~6–10%) of the monooxidized compound which is "doped" into the dioxidized salts. [g] See ref 13. [h] See R. H. Herber, *Inorg. Chem.*, **8**, 174 (1969); G. K. Wertheim and R. H. Herber, *J. Chem. Phys.*, **38**, 2106 (1963); T. Birchall and I. Drummond, *Inorg. Chem.*, **10**, 399 (1971).

center doublet. The temperature dependence depicted in Figure 1 appears to be due to a loss of some intensity in these shoulders. The solid lines in both Figures 1 and 2 are the least-squares fit lines, fit in each case to *three* quadrupole-split doublets. The fitting parameters are given in Table II as well as the approximate relative amount of the two species. However, an evaluation of relative amounts of the two species by such fittings could be in error, because the site from which this third doublet originates could have a different recoilless fraction than the other two iron centers of the mixed-valence species. It is tempting to assign the third doublet to the average-valence cation. A loss of average-valence signal with

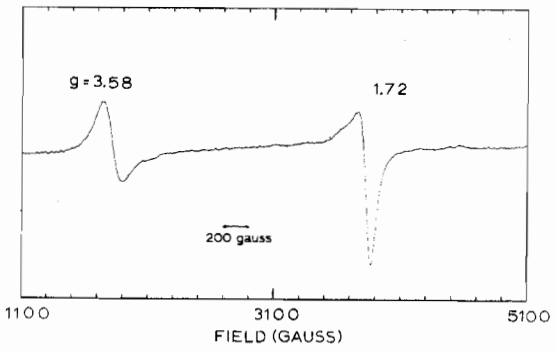

Figure 3. X-Band (9.167 GHz) EPR spectrum of a powdered sample of biferricenium$^+I_3^-$ at 12°K.

decreasing temperature has been noted in some other iron[28,29] and europium[30] mixed-valence systems. The third quadrupole doublet seen for biferricenium$^+$TCA$^-$·2TCAA is *not* due to dioxidized material, because biferricenium$^{2+}(BF_4^-)_2$ has been reported[7] to have a quadrupole splitting similar to simple ferricenium salts. The analytical data in Table I make it improbable that the third doublet is due to an impurity. It is clear to us that both the compound preparation and the Mössbauer results are reproducible. It is possible that there are two crystalline forms of biferricenium$^+$TCA$^-$·2TCAA in our sample. X-Ray structural work is needed to ascertain the conformation and structural characteristics of the biferricenium(1+) ion as it is found in the picrate, triiodide, and trichloroacetate salts.

Variable-temperature (4.2–290°K) susceptibility data have already been reported[16] for the dioxidized biferrocene salt, biferricenium$^{2+}(DDQH^-)_2$, and it was found that the μ_{eff}/Fe vs. temperature curve looked identical with that obtained for either ferricenium$^+$DDQH$^-$ or ferricenium$^+I_3^-$. The μ_{eff} value is relatively constant down to 20–30°K whereupon there is a smooth decrease in μ_{eff} by 0.2–0.4 BM to the 4.2°K value. In our previous paper[16] we elected to fit by least squares the data to *perturbation* equations appropriate for the two Kramers doublets from the $^2E_{2g}((a_{1g})^2(e_{2g})^3)$ state and the Kramers doublet from the $^2A_{1g}((a_{1g})^1(e_{2g})^4)$ state. Reasonable fits to the data could be found using a low-symmetry distortion parameter $\delta = \langle e_{2g}^+|H_{eff}|e_{2g}^-\rangle$, an orbital reduction parameter k', an energy separation parameter $\Delta E = E(^2A_{1g}-^2E_{2g})$, and a Curie–Weiss constant Θ. The ΔE values from the fitting were found to be large (>2300 cm^{-1}) and as such it should be emphasized that, *contrary* to the findings of the earlier paper[3] on the magnetism of ferricenium systems, there is *no* need to invoke appreciable thermal population in the $^2A_{1g}$ doublet (also there is no need for temperature dependence in δ, as proposed) and the $^2A_{1g}$ state influences the magnetism only through second-order effects.

Partially as a result of the very recent paper by Anderson and Rai[32] and as a result of data to be presented we have modified our theoretical model and, as detailed in the Appendix, instead of a perturbation treatment, the simplex minimization routine is used in conjunction with diagonalizations of the three energy matrices for the three static magnetic field orientations. The matrices include such parameters as the orbital reduction parameter k', the energy separation parameter ΔE (between baricenters of $^2E_{1g}$ and $^2A_{1g}$), and the low-symmetry distortion parameter δ as defined above. The matrices also contain terms for the configuration interaction of the $^2E_{2g}$ state with the $^2A_{1g}$ state (E' in D_5' symmetry) and the two lowest energy $^2E_{1g}$ excited states with the parameters $\epsilon = \langle e_{2g}|H_{eff}|a_{1g}\rangle$ and $\sigma = \langle e_{2g}^{\pm}|H_{eff}|e_{1g}^{\mp}\rangle$, respectively.

We have recorded the 12°K X-band powder EPR spectra for the I_3^- (see Figure 3) and TCA$^-$·2TCAA salts of biferricenium(1+) and the DDQH$^-$ salt of biferricenium(2+) (see Figure 4); the results are summarized in Table III along with those reported by Cowan. Variable-temperature (2–300°K) magnetic susceptibility data have been recorded by Cowan[8] for biferricenium picrate and they are illustrated in Figure 5. The fitting procedure described in the Appendix was used to fit the ferricenium and biferricenium data given in Table III. When available for a given compound, both the EPR and variable-temperature magnetic susceptibility were simultaneously fit. The resulting k', ΔE, δ, ϵ, and σ parameters are given in Table IV.

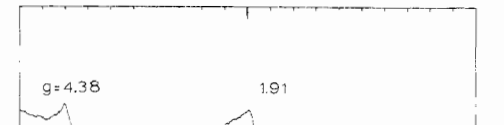

Figure 4. X-Band (9.181 GHz) EPR spectrum of a powdered sample of biferricenium$^{2+}(DDQH^-)_2$ at 12°K.

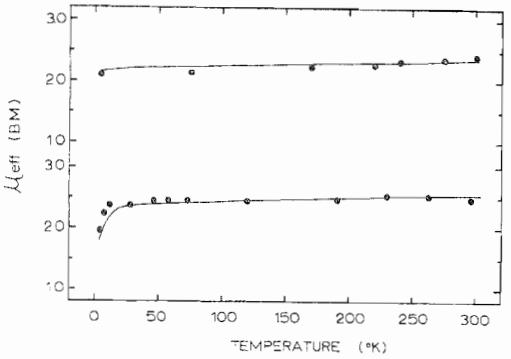

Figure 5. Effective moment (μ_{eff} per iron atom) vs. temperature curves: bottom, ferricenium$^+I_3^-$; top, biferricenium picrate. The data are from ref 16 and 8, respectively, and the solid lines are theoretical lines fit by least-squares to the model presented in the Appendix.

As can be seen from Table IV, fitting the ferricenium triiodide and biferricenium(1+) data show, as in our previous[16] perturbation analysis, that the $^2A_{1g}$ state is well above the ground state with $\Delta E > 900$ cm^{-1}. The biferricenium$^+$ systems are appreciably more distorted (as judged by the δ parameters) than the ferricenium ion in $Fe(cp)_2^+I_3^-$ and this is not unexpected due to the bulky nature of the ferrocenyl substituent. The larger distortion and, thus, less orbital angular momentum in the ground state of the biferricenium(1+) ion accounts for the fact that the biferricenium(1+) EPR signals are easier to obtain than those for the ferricenium ion. The biferricenium(1+) EPR spectra are apparently axial; however, the broadness of the perpendicular signal is to be noted. It is also noted that the biferricenium(1+) fittings require very small ϵ parameters and negligible σ parameters, whereas, the ferricenium data are fit with $\epsilon = 52$ cm^{-1} and negligible σ. The $\delta = 52$ cm^{-1} parameter means that there is a small mixing of the $^2A_{1g}$ Kramers doublet with those from the $^2E_{1g}$ state.

Fitting of the EPR and susceptibility data for biferricenium$^{2+}(DDQH^-)_2$ gives parameters similar to those for ferricenium triiodide. By far the biggest difference between biferricenium(2+) and the ferricenium and biferricenium(1+) ions is that the $^2A_{1g}$ state has moved to lower energy. It should be pointed out (see Table IV) that our EPR data on biferricenium$^{2+}(DDQH^-)_2$ are different from Cowan's data[7] on

Table III. Electron Paramagnetic Resonance Data

Compd	T, °K	Sample condition[a]	g_1 (g_{11})[b]	g_2 ($g_\perp$)[b]	g_3 ($g_\perp$)[b]
Ferricenium$^+I_3^-$ [c]	20	Glass	4.35		1.26
Biferricenium$^+I_3^-$	12	Solid	3.58		1.72
Biferricenium$^+$TCA$^-$·2TCAA	12	Solid	3.34		1.86
Biferricenium picrate[d]	77	Glass	3.53		1.85
Biferricenium^{2+}(DDQH$^-$)$_2$[e]	298	Solid	4.25		2.01
	77	Solid	4.27		2.02
	12	Solid	4.38		1.91
Biferricenium^{2+}(BF_4^-)$_2$[d]	298	Solid	3.2		1.91
1′,6′-Diiodobiferricenium$^+I_3^-$	77	Solid	2.79		2.02
	12	Solid	2.75	2.01	1.97
Biferricenylenium$^+I_5^-$	298	Solid	2.33		1.99
	77	Solid	2.34	1.99	1.88
	12	Solid	2.36	1.99	1.91
	77	Glass	2.30	2.10	1.92
Biferricenylenium$^+I_2^-$	298	Solid	2.37		2.02
	77	Solid	2.36		2.04
	12	Solid	2.34	2.01	1.88
Biferricenylenium$^+PF_6^-$	298	Solid	2.33	2.02	1.88
	77	Solid	2.32	2.02	1.88
	12	Solid	2.33	2.02	1.88
	298	(Doped)	2.31	2.00	1.87
Biferricenylenium$^+$DDQH$^-$	298	(Doped)	2.35	2.02	1.92
	77	(Doped)	2.39	2.02	1.91
1,12-Dimethyl[1.1]ferricenophamium$^+I_3^-$	12	Solid	4.28	2.07	2.03
1,12-Dimethyl[1.1]ferricenophanium$^+$DDQH$^-$	77	(Doped)	4.25	2.05	1.94

[a] All glasses are acetone; certain singly oxidized species were found doped at low concentrations in the dioxidized compound. [b] g_2 and g_3 are the perpendicular signals; however when unsplit it is given as g_3. The parallel signal is given as g_1. [c] See ref 32 and 36. [d] See ref 8. [e] The widths at half-height for the parallel signals at the three temperatures are 200, 100, and 60 G, respectively; values for the perpendicular signals are 490, 400, and 150 G, respectively.

Table IV. Ligand Field Fitting Parameters[a]

Compd	Compd state	k'	δ, cm^{-1}	Δ, cm^{-1}	ϵ, cm^{-1}	σ,[b] cm^{-1}
Ferricenium$^+I_3^-$ [c]	Glass, 20°K	0.76	280	>~900	50	
Biferricenium$^+I_3^-$	Solid, 12°K	0.77	583	>~900	5	
Biferricenium$^+$TCA$^-$·2TCAA	Solid, 12°K	0.92	1049	>~900	4	
Biferricenium picrate[d]	Glass, 77°K	1.00	1107	>~930	4	
Biferricenium^{2+}(DDQH$^-$)$_2$[e]	Solid, 12°K	1.00	636	−96	57	~100
Biferricenium^{2+}(BF_4^-)$_2$[d]	Solid, 298°K	0.98	1358	>~650	39	
1′,6′-Diiodobiferricenium$^+I_3^-$	Solid, 12°K	0.95	2065	−1744	31	~100
Biferricenylenium$^+PF_6^-$	(Doped), 12°K	0.28	465	−253	60	~100
1,12-Dimethyl[1.1]ferricenophanium$^+I_3^-$	Solid, 12°K	1.00	685	−95	58	~100

[a] EPR and, when available, variable-temperature magnetic susceptibility data were used in the least-squares theoretical fit; see the Appendix for details of fitting. [b] Accurate values of this parameter were difficult to determine from the fitting program. [c] Susceptibility data for this compound are available from ref 16 and 32. [d] Susceptibility data from ref 8. [e] Susceptibility data from ref 16.

biferricenium^{2+}(BF_4^-)$_2$. Also, we found little temperature dependence in our EPR in contrast to Cowan's report. In short, the EPR and susceptibility for biferricenium(1+) and biferricenium(2+) are not terribly different from those for the ferricenium ion. There are indications of increases in the δ distortion parameters and perhaps some movement in the relative position of the $^2A_{1g}$ state.

The electronic absorption data for various biferrocene systems are summarized in Table V. The electronic spectrum of biferrocene, as well as those for biferrocenylene and the [1.1]ferrocenophanes (vide infra), is essentially identical with that for ferrocene. At room temperature there are two bands in the visible region which can be assigned as d–d transitions based on their position and intensity. The lower energy band is probably composed of two transitions ($a^1E_{1g} \leftarrow {}^1A_{1g}$ and $^1E_{2g} \leftarrow {}^1A_{1g}$) as has been shown[33] with low-temperature measurements for ferrocene. The higher energy band is associated with the $b^1E_{1g} \leftarrow {}^1A_{1g}$ transition. The lower energy band is not resolved for biferrocene, biferrocenylene, or the [1.1]ferrocenophanes. The room-temperature band positions move to lower energies in the series ferrocene > biferrocene > biferrocenylene. When estimates are placed on the positions of the two lowest energy transitions from the asymmetric unresolved lower energy band (a Du Pont curve analyzer was used) and the data are analyzed with the d^6 equations,[33] the ligand field parameters listed in Table VI result. In the series ferrocene, biferrocene, and biferrocenylene the difference in core energies (e_{2g}–a_{1g}) decreases and the ring–metal covalency, as indicated by the electron repulsion parameter B, apparently increases. The three uv biferrocene bands can be assigned as ligand-to-metal (L → M) transitions at 295 and 218 nm and a M → L transition at 265 nm by analogy to ferrocene.

Theoretically, there should be seven d–d transitions for the ferricenium ion, all of which should fall in the visible and near uv regions. Only four of these have been found and none of them have been assigned with certainty.[33] Ferricenium also has a $^2E_{1u} \leftarrow {}^2E_{2g}$ charge-transfer[34,35] transition at 16,200 cm^{-1} with $\epsilon = 450\ M^{-1}$ cm^{-1}. In contrast to the ferricenium case, where there are at least five bands in the visible region, there are only three bands in the visible spectrum of biferricenium(1+) (see Table V). The bands at 14,300 and 18,500 cm^{-1} are probably attributable to the ferricenium half of the biferricenium(1+) molecule, as no transitions occur below 22,200 cm^{-1} for biferrocene or ferrocene. The quite broad band at 14,300 cm^{-1} is a good candidate for the "hole" transition ($^2E_{1u} \leftarrow {}^2E_{2g}$) which has moved to lower energy than the ferricenium 16,200-cm^{-1} position due to substitutional effects. The ferricenium band system has been reported[33–35] to show a dramatic resolution of vibrational structure at low temperatures (77–4.2°K). We have carried out low-temperature electronic absorption measurements on the TCA$^-$·2TCAA salt of biferricenium(1+) and have found no

Table V. Electronic Absorption Data for Biferrocene Systems at Room Temperatures

Compd	$h\nu_{max}$, nm	$h\nu_{max}$, cm^{-1}	$\epsilon, M^{-1}\ cm^{-1}$	$\Delta E_{1/2}$,[g] cm^{-1}
Biferrocene[a]	450	22,200	522	
	345	29,000 sh	698	
	295	33,900	6,780	
	265	37,700 sh	7,070	
	218	45,800	41,700	
Biferricenium$^+I_3^-$[b]	1960	5,100	541	3950
	700	14,300 sh		
	542	18,450	2,030	
	360[c]	27,800	13,500	
	291[c]	34,400	31,200	
	245	40,800	30,900	
	<210	>48,000		
Biferricenium$^+TCA^-\cdot 2TCAA$[b,d]	1830	5,460		4400
	700	14,300 sh		
	540	18,500		
	350	28,600		
	294	34,000		
	245	40,800		
	<210	>48,000		
Biferricenium picrate[b,e]	1900	5,260	551	~4000
	700	14,300 sh		
	542	18,500	1,860	
	374[f]	26,700		
	300	33,300	8,570	
	245	40,800 sh	47,000	
	<210	>48,000		
1′,6′-Diiodobiferricenium$^+I_3^-$[b]	1840	5,430	[h]	~4000
	670	14,900 sh	[h]	
	537	18,600	[h]	
	360[c]	27,800	23,800	
	295[c]	33,900	67,400	
	243	41,200	96,600	
	<210	>48,000		
Biferricenium$^{2+}(DDQH^-)_2$[i]	800[j]	12,500		
	500[k]	20,000		
	350	28,600 sh		

[a] Ethanol solution. [b] Acetonitrile solution. [c] These bands are absorptions by I_3^- as per A. I. Popov and R. F. Swensen, *J. Am. Chem. Soc.*, 77, 3724 (1955). [d] Methanol solution. [e] Reference 5. [f] Picrate anion absorption. [g] Bandwidths estimated at the point where $I_\nu\nu_{max}/I_{max}\nu = 1/2$. [h] Not soluble enough to determine these accurately. [i] KBr pellet (bands in the uv region were unresolved). [j] DDQ (dichlorodicyanoquinone) anion absorption. [k] This band develops a shoulder at 77°K, $\bar{\nu} = 20{,}700\ cm^{-1}$, and the maximum shifts to 19,800 cm^{-1}.

Table VI. Spin-Allowed Ligand Field Absorption Transitions and Parameters for d^6 Metallocenes[a]

	Ferrocene	Biferrocene	Biferrocenylene	[1.1]Ferrocenophanes
$^1A_{1g} \rightarrow a^1E_{1g}$	21,800	21,200	20,500[b]	21,800[b]
$^1A_{1g} \rightarrow {}^1E_{2g}$	24,000	23,500[b]	22,800[b]	24,100[b]
$^1A_{1g} \rightarrow b^1E_{1g}$	30,800	29,000	27,800	31,300
Δ_2[c]	22,000	21,200	20,500	22,000
Δ_1[c]	−7,100	−6,490	−6,210	−7,460
B	390	323	297	412
β	0.42	0.35	0.32	0.44

[a] All numbers except β are in cm^{-1}. [b] These numbers are estimated from an unresolved band based on the values found for ferrocene. [c] $\Delta_1 = \epsilon^c(e_{2g}-a_{1g})$; $\Delta_2 = \epsilon^c(e_{1g}-a_{1g})$, where ϵ^c are core one-electron energies.

vibrational structure in Nujol mulls or KBr pellets down to 20°K. The biferricenium(1+) band does narrow somewhat and is resolved from the higher energy band at low temperatures. The approximately threefold increase in intensity of the biferricenium(1+) "hole" transition was taken by Cowan and Kaufman[5] to "indicate that the two ring systems are not entirely isolated and that there is some interaction of the ferrocenium chromophore by the adjacent ferrocene ring". In our opinion, the increased intensity could be largely the result of the greater distortion in the biferricenium(1+) ion.

As can be seen in Table V and Figure 6 no electronic transitions occur at wavelengths greater than ~800 nm for biferricenium$^{2+}(DDQH^-)_2$. Only two nonanion bands can be seen in the visible region; the uv spectrum was not run because the sample was pelleted in KBr of necessity because the biferricenium^{2+} ion is reported[15] to convert rapidly to the monooxidized form in solution, a fact that we verified. The

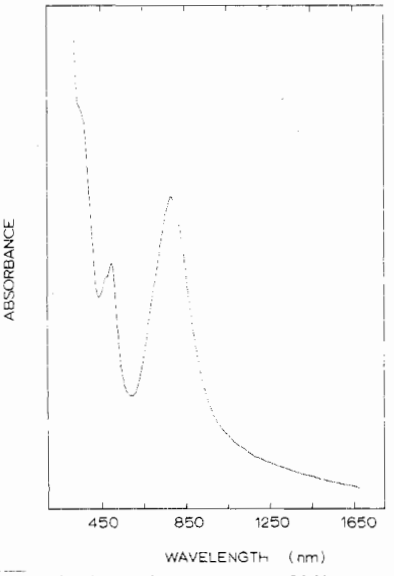

Figure 6. Electronic absorption spectrum of biferricenium^{2+}-$(DDQH^-)_2$ in a KBr pellet at 77°K. The strong absorption at 800 nm (12,500 cm^{-1}) is due to the anion $DDQH^-$.

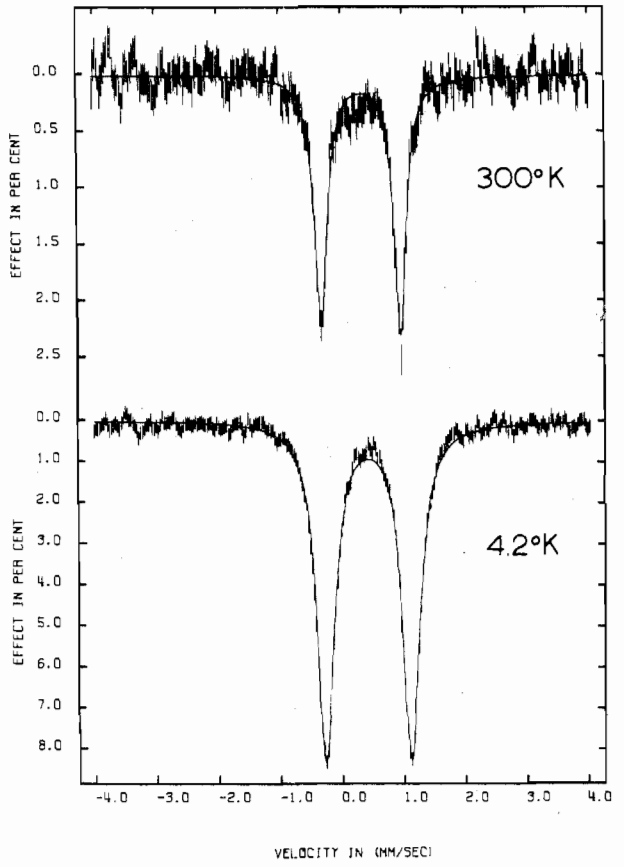

Figure 7. ^{57}Fe Mössbauer spectra for 1′,6′-diiodobiferricenium^{+}-I_3^- at 300 and 4.2°K. The velocity scale is referenced to the Co in Rh source.

two biferricenium(2+) bands are probably similar in origin to those found for biferricenium(1+) at similar energies. The biferricenium^{2+} ion does *not* have a near-ir band as is found for the mixed-valence biferricenium(1+) ion. This near-ir band, of course, has been assigned to the intervalence transfer band.

1′,6′-Diiodobiferrocene. The ring substitutions present in 1′,6′-diiodobiferricenium(1+), cation II with $n = 1$, should be sufficient to effect a change in the properties of the compound. We have prepared the triiodide salt of this cation, and the 300 and 4.2°K Mössbauer spectra in Figure 7 each show only one quadrupole-split doublet. Thus, the two iron atoms are equivalent on the Mössbauer time scale and the intervalence-transfer rate is greater than $\sim 10^7$ sec^{-1}. It is notable that the quadrupole splitting (1.284 mm/sec at 300°K, see Table II for fitting data) is intermediate between that found for the Fe(II) and Fe(III) sites in biferricenium and that the 1.284 (6) mm/sec ΔE_Q value is not unlike the ΔE_Q value of 0.903 (29) mm/sec obtained for the third doublet ("average-valence" species?) in the 300°K spectrum of biferricenium^{+}TCA^{-}·2TCAA. The iodine ring substitution in conjunction with a triiodide counterion has resulted in an increased electron-transfer rate in cation II, $n = 1$, over that in cation I, $n = 1$. Unfortunately, we do not, at present, know what structural changes have resulted from the iodine disubstitution. It may be argued that the overall bulkiness of cation II, $n = 1$, is such that, in order for it to pack with triiodide ions, it is in the cis conformation as depicted above (i.e., structure II). In this case direct iron–iron electron exchange could be facilitated. On the other hand, perhaps *intramolecular* repulsions lead to a trans conformation as depicted in V. If this is the case, the increased electron-transfer rate over that in the unsubstituted biferricenium(1+) salts

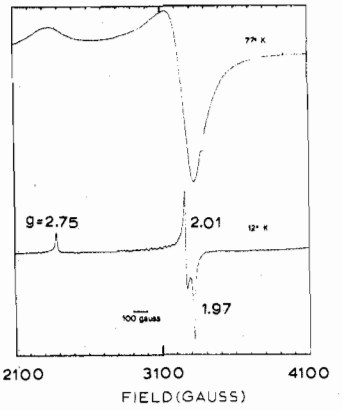

Figure 8. X-Band (9.112 GHz) EPR spectra of a powdered sample of 1′,6′-diiodobiferriconium$^{+}I_3^-$ at 77 and 12°K.

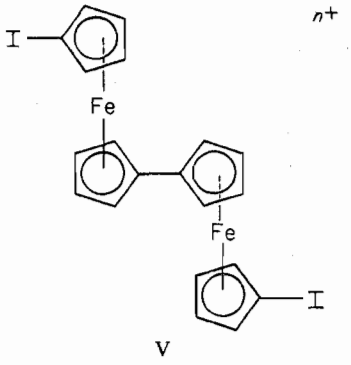

V

could be the result of a situation where the 1′,6′-diiodobiferricenium(1+) cation has the trans structure (V) and the biferricenium(1+) cation has a structure intermediate between the cis and trans structures. Any inter-ring propagation of electron exchange would probably be attenuated in such an intermediate conformation (vide infra).

With the discovery that cation II, $n = 1$, is of the average-valence type on the ^{57}Fe Mössbauer time scale it became desirable to determine the other physical properties of 1′,6′-diiodobiferricenium triiodide. In contrast to the EPR spectrum of biferricenium$^{+}I_3^-$, the spectrum of the triiodide salt of cation II, $n = 1$, shown in Figure 8, is characteristic of a species with a relatively isotropic **g** tensor. It is also considerably easier to obtain the EPR signal of this disubstituted biferricenium(1+) compound in comparison to ferricenium(1+) and unsubstituted biferricenium systems which can only be seen in the case of powdered pure solids at low temperatures such as ~10°K. Figure 8 shows that a powdered pure solid sample of the I_3^- salt of cation II, $n = 1$, readily gives an EPR spectrum at 77°K. Furthermore, the signals for cation II, $n = 1$, appreciably sharpen upon cooling the sample to 12°K whereupon the $g_\perp$ signal is resolved into $g_x = 1.97$ and $g_y = 2.01$ signals with $g_z = 2.75$. The ferricenium ion (I_3^- salt) has a considerably more anisotropic **g** tensor with $g_\parallel = 4.35$ and $g_\perp = 1.26$.[36] The anisotropic **g** tensor of the ferricenium ion has been shown to be interpretable in terms of an $^2E_{2g}$ ground state which is split into two Kramers doublets (E″ and A′, A″ in the double group D_5') by spin–orbit coupling and crystal fields of symmetry lower than D_5.[31,32,36-38] The low-symmetry crystal fields also mix E″ and (A′, A″).

The relatively isotropic **g** tensor of 1′,6′-diiodobiferricenium$^{+}I_3^-$ is similar to that for delocalized, average-valence biferricenylenium(1+) (see Table III) and we conclude that the thermal electron-transfer rate in 1′,6′-diiodobiferricenium$^{+}I_3^-$ is faster than the EPR time scale; thus k(thermal) > ~10^9 sec^{-1}. This is, of course, some 2 orders of magnitude faster rate than is seen for the unsubstituted bi-

ferricenium(1+) ion. An upper limit on k(thermal) for 1',6'-diiodobiferricenium$^+I_3^-$ is presently not known and as such it cannot be concluded that the single unpaired electron is completely delocalized as appears to be the case for biferricenylenium(1+) (vide infra). If the interaction between the two iron ions in 1',6'-diiodobiferricenium(1+) is not very large (in theory only a relatively weak interaction is needed to establish an appreciable thermal electron-transfer rate), then it is still possible to use ligand field theory, as we did above for biferricenium(1+), to assess the electronic structure at the Fe(III) center. As Table IV shows, a fit of the relatively isotropic **g** tensor of 1',6'-diiodobiferricenium(1+) is obtained wherein the $^2A_{1g}$ ferric excited state is placed quite close in energy to the lowest Kramers doublet from the $^2E_{2g}$ state. It is not claimed that the set of parameters given in Table IV is unique. It is probably also possible to get a local minimal fit wherein the orbital reduction factor k' is small. In other words, a quenching of orbital angular momentum (small k') or a low-lying $^2A_{1g}$ excited state is required to fit the isotropic **g** tensor with the ligand field theory presented in the Appendix. It must be cautioned that if the interion interaction is relatively large and 1',6'-diiodobiferricenium(1+) is totally delocalized, then a ligand field approach as formulated is inappropriate and molecular orbital machinery is needed.

In spite of the fact that the 1',6'-diiodobiferricenium(1+) ion has a considerably greater thermal intervalence transfer rate than that for the biferricenium(1+) ion, the electronic absorption spectra of the two are nearly identical (see Table V). There is some slight shifting of the 1',6'-diiodobiferricenium(1+) bands to lower energy, but this is probably due to the substitutional effects of the iodine atoms. The most notable band observed for this substituted biferricenium(1+) ion is the "intervalence-transfer" band at 1840 nm. Such a band is also seen for the totally delocalized biferricenylenium(1+) ion and an explanation is given below. We have also found one additional property of 1',6'-diiodobiferrocene that closely parallels that of biferrocene. The molecule 1',6'-diiodobiferrocene dissolved in acetonitrile exhibits two one-electron reversible oxidation half-waves at 0.42 and 0.70 V vs. the SCE employing a rotating platinum electrode. The corresponding biferrocene values under the same conditions are 0.31 and 0.64 V vs. the SCE, while biferrocenylene (III, $n = 0$) shows two waves at 0.13 and 0.72 V vs. the SCE.[16]

Biferrocenylene Systems. Six papers[12-17] have already appeared with data bearing on the biferrocenylene system. The reported ^{57}Fe Mössbauer and X-ray photoelectron work on biferricenylenium(1+), that is, cation III, $n = 1$, has shown that this doubly fused system is an average-valence system. The thermal intervalence transfer rate is so great ($>\sim 10^{17}$ sec^{-1}) that only a single type of iron center is discernible with XPS.[13] It should be mentioned that the XPS results on these mixed- and average-valence biferrocene-like compounds have experienced some criticism.[39] In this vein it should be noted that we feel the ^{57}Fe Mössbauer determinations are above reproach. During this work, in fact, we have seen Mössbauer signals from small amounts of biferricenylenium(1+) doped into the PF_6^- and $DDQH^-$ salts of biferricenylenium(2+). Table II shows that the fitting parameters for these species are in agreement with those reported for the I_5^- and picrate salts of biferricenylenium(1+).

Electronic absorption data for various biferrocenylene systems are collected in Table VII. The electronic spectra of biferricenylenium(1+) and biferricenium(1+) in the visible and uv regions are very similar. The band at ~600 nm can be assigned as the "hole" transition. This assignment was originally made by Mueller-Westerhoff and Eilbracht[14] when they first communicated that this doubly fused ion is of the *mixed-valence* type. In a later paper[15] they indicated that

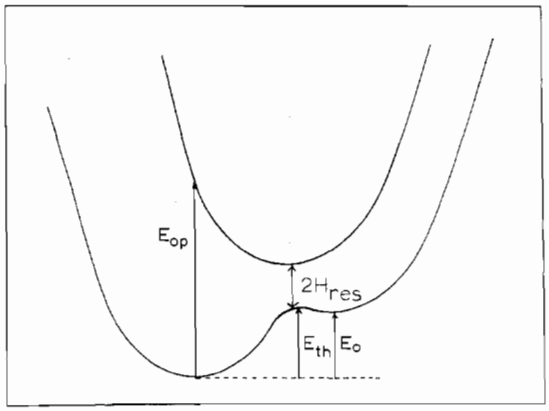

Figure 9. Potential well diagram for a mixed-valence system.

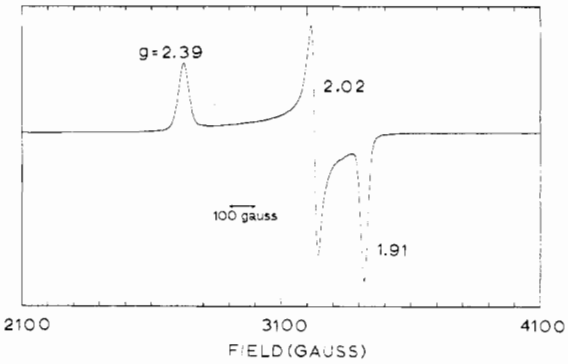

Figure 10. EPR spectrum of biferricenylenium$^+$ ion doped at 12% (as determined by ^{57}Fe Mössbauer spectroscopy) into diamagnetic biferricenylenium$^{2+}(DDQH^-)_2$; run as a solid at 77°K and 9.105 GHz.

perhaps the biferricenylenium(1+) ion is delocalized (i.e., average valence); however, they were puzzled as to how such a delocalized system could have a "hole" transition. Figure 9 depicts in a familiar and probably overly simplified way the double-well character of the ground state of this ion. The E_{th} barrier in this case is small enough to allow at room temperature a very appreciable intervalence-transfer rate. At some ~16,000 cm^{-1} higher energy there is probably a complicated double-well system representing the formerly Fe(III) localized $^2E_{1u}$ excited state which could now also be delocalized. In short, there can still be an electronic transition wherein an electron is excited from a one-electron orbital that is largely ring in character to an orbital that is largely metal d orbital in character. We have studied the electronic spectrum of a sample of biferricenylenium$^+$TCA$^-$·2TCAA pelleted in KBr at temperatures approaching 20°K; the ~600-nm "hole" transition does not show any vibrational structure at low temperatures. In comparison to the simpler ferricenium ion case the complexity of the biferricenylenium(1+) wells must preclude any improvement in resolution.

As can be seen from Table III and Figure 10 the biferricenylenium(1+) ion has a three-g-value spectrum wherein the g values are relatively isotropic (g_1 = 2.30–2.39, g_2 = 1.99–2.10, and g_3 = 1.88–1.92) and are not very anion or solution dependent. The EPR spectrum that we previously reported[16] for biferricenylenium$^+I_3^-$ (which was really the I_5^- salt) shows many small features between g_1 and g_2 and these features have now been identified as being due to incomplete powder averaging of the microcrystalline sample. This was confirmed by (1) rotation of the tube which caused the peaks to shift in position and intensity and (2) thorough grinding of the material to give a powder which no longer showed these low-intensity peaks in the EPR spectrum.

The magnetic susceptibility also reflects the isotropic nature

Table VII. Electronic Absorption Data for Biferrocenylene Systems at Room Temperature

Compd	$h\nu_{max}$, nm	$h\nu_{max}$, cm^{-1}	$\epsilon, M^{-1}\ cm^{-1}$	$\Delta E_{1/2}$,[a] cm^{-1}
Biferrocenylene[b]	466	21,500	255	
	360	27,800	563	
	218	46,000		
Biferricenylenium$^+I_5^-$ [c]	1470	6,790	1,710	3250
	601	16,600	583	
	471	21,200 sh	1,110	
	358[h]	27,900	7,190	
	336	29,800 sh	6,650	
	288[h]	34,700		
	245	40,800		
	<210	>48,000		
Biferricenylenium$^+PF_6^-$ [c]	1510	6,640	1,930	3600
	594	16,800	417	
	466	21,500	1,140	
	329	30,400	5,150	
	269	37,200	10,600	
	239	41,800	14,600	
	<210	>48,000		
Biferricenylenium$^+BF_4^-$ [c,d]	1550	6,450	2,100	3600
	600	16,700	370	
	466	21,500	1,000	
	333	30,000	6,170	
	269	37,200	17,800	
Biferricenylenium picrate[c-e]	1550	6,670	1,800	3600
	600	16,700 sh	370	
	269	37,200	36,000	
Biferricenylenium$^{2+}(TCNQ^-)_2$ [e,f]	1500	6,670	1,600	
Biferricenylenium^{2+} [g,i]	466	21,500	708	
	426	23,500	785	
	411	24,300 sh	~600	
	344	29,100 sh	~4,000	
	271	36,900	17,600	
	237	42,200	14,100	
	<210	>48,000		

[a] Bandwidths were estimated at the point where $I_\nu \nu_{max}/I_{max}\nu = 1/2$. Each of the near-infrared bands is actually composed of two bands; see text. [b] Chloroform solution. [c] Acetonitrile solution. [d] Reference 14; not all bands listed in article. [e] Reference 12; not all bands listed in article. [f] DMF solution. [g] Concentrated sulfuric acid solution at room temperature. [h] These bands are probably due to absorptions by $I_3^- + I_2$ as per A. I. Popov and R. F. Swensen, *J. Am. Chem. Soc.*, 77, 3724 (1955). [i] The DDQ (dichlorodicyanoquinone) salt shows one transition, other than those due to the anion, at 20,800 cm^{-1}. Bands at higher energies were not resolved due to dispersion in the KBR pellet. These data are consistent with those found by Mueller-Westerhoff.[15]

Table VIII. Variable-Temperature Magnetic Susceptibility Data for Two Biferrocenylene Systems[a]

T, °K	$10^3\chi_M^{cor}$,[b] cgsu/mol: Biferricenylenium$^+I_5^-$	Biferricenylenium$^{2+}(DDQH^-)_2$
119	3.64	
80		2.02
46.7	10.2	
18.4	23.6	
12.2	37.7	16.6
8.6	54.6	
5.8	80.0	
4.5	96.9	30.0
μ_{eff}(av)	1.90 BM	0.8 BM

[a] Both compounds show Curie-law behavior. [b] Molar paramagnetic susceptibilities are corrected for background and for the diamagnetism of the compound; the latter are from Pascal's constants and the values are as follows: biferricenylenium$^+I_5^-$, -466.9×10^{-6} cgsu; biferricenylenium$^{2+}(DDQH^-)_2$, -429.2×10^{-6} cgsu.

of the biferricenylenium(1+) **g** tensor with the picrate and BF_4^- salts being reported[13] to be Curie law type with a room-temperature μ_{eff} of 1.88 BM. We have carried out susceptibility measurements on biferricenylenium$^+I_5^-$ from 4.5 to 119°K and have also found it to be Curie law type with an μ_{eff} of 1.90 BM; the data are given in Table VIII. The EPR and susceptibility data for only one anion were least-squares fit to the crystal field model and the resultant parameters for one "fit" are given in Table III. As was found for the 1',-

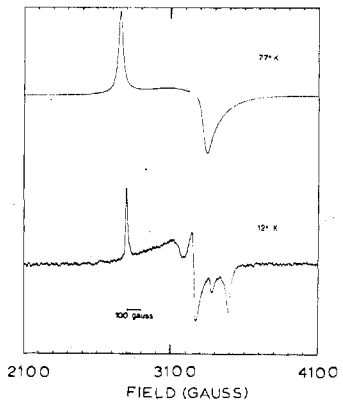

Figure 11. X-Band EPR spectra of a solid sample of biferricenylenium$^+I_2^-$ at 77 and 12°K.

6'-diiodobiferricenium(1+) ion, the crystal field fitting requires (1) the orbital angular momentum of the "hole" to be greatly quenched over the situation in biferricenium(1+) or ferricenium(1+) systems as reflected by the small values of k' and (2) the $^2A_{1g}$ state to move closer in energy to the ground state.

There are some anomalous features in the 12°K EPR spectra of two of the four biferricenylenium(1+) systems. The 12°K X-band spectrum of the small amount of biferricenylenium(1+) doped into a sample of biferricenylenium$^{2+}(PF_6^-)_2$ shows some additional splitting in the g_2 signal. The 12°K X-band spectrum of a powdered sample of biferricenyleni-

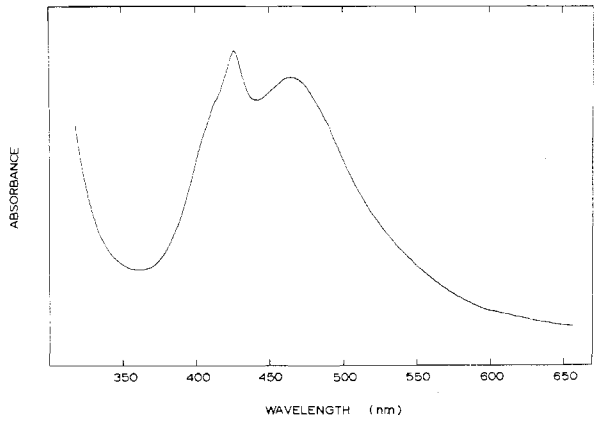

Figure 12. Electronic absorption spectrum of biferricenylenium(2+) in concentrated sulfuric acid at room temperature.

Scheme I

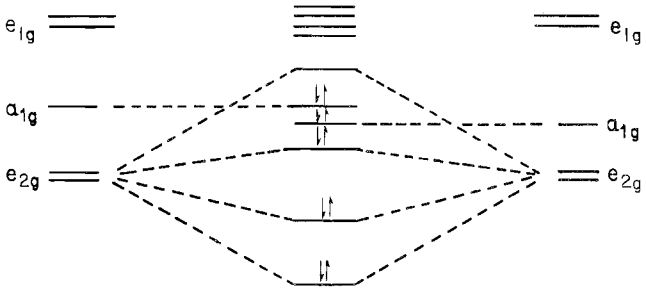

um$^+$I$_2^-$, reproduced in Figure 11, shows that not only are the three g values resolved at the low temperature but also an additional peak (g = 1.94) is seen between g_2 and g_3. We do not have an explanation for these anomalous features. It is clear that at 12°K there would not be enough population in the higher energy $^2E_{2g}$ Kramers doublet for it to give an EPR signal.

As has been reported,[16] the case of biferricenylenium(2+) is most interesting. When biferrocenylene is dioxidized with DDQ or concentrated sulfuric acid, the resulting DDQH$^-$ and PF_6^- salts are *diamagnetic*. We have now measured the magnetic susceptibility of our sample of biferricenylenium^{2+}-(DDQH$^-$) at 293, 80, 12.2, and 4.5°K and have found the compound to have a small residual paramagnetism with μ_{eff} = 0.8 BM. This small moment is most likely a result of a small amount of biferricenylenium(1+) (which we have seen in the ^{57}Fe Mössbauer spectrum) in conjunction with temperature-independent paramagnetism which could be the major contributor because of the availability of low-lying excited states.

There are no electronic absorptions at energies below 21,500 cm^{-1} in the spectrum of biferricenylenium(2+) (see Table VII and Figure 12). To individuals very accustomed to investigating the fine detail of the $^2E_{1u} \leftarrow {}^2E_{2g}$ "hole" transition in various ferricenium systems,[33-35] the most startling result is the absence of a band assignable to the hole transition. With the knowledge that the compound is diamagnetic, the lack of a hole transition is understandable. If the d orbitals of the two ferricenium ions in biferricenylenium^{2+} interact to some extent, an MO diagram results (see Scheme I). The exact ordering of the lowest six orbitals is not important, but the important point is that in this diamagnetic complex there is not a "hole"-type orbital, and, as such, excitation of an electron from a ring orbital into the hole is not possible. The above d orbitals are, of course, mixed to a certain degree with cyclopentadiene ring orbitals and the degree to which this occurs determines the extent to which the above interactions are the result of superexchange, i.e., overlap of electron density propagated via the cyclopentadienyl rings. A priori, this does not seem to be too feasible because an unpaired electron on a ferricenium ion is to be found in an e_{2g} symmetry ($d_{x^2-y^2}$, d_{xy}) orbital (D_{5d} symmetry) and this orbital is most assuredly nonbonding. It must be remembered, however, that the interaction we are dealing with is weak and all that is required for biferricenylenium(2+) to be diamagnetic up to room temperature is that the unpaired electron state, the triplet state of the ion, lie in excess of ~400 cm^{-1} (1.5 kcal/mol) above the diamagnetic ground state. In fact, the $d_{x^2-y^2}$ and d_{xy} orbitals on each Fe(III) are directed such that a very weak *direct* Fe–Fe interaction (overlap) is possible even though the Fe–Fe distance in the unoxidized biferrocenylene is known[40] to be 3.98 Å.

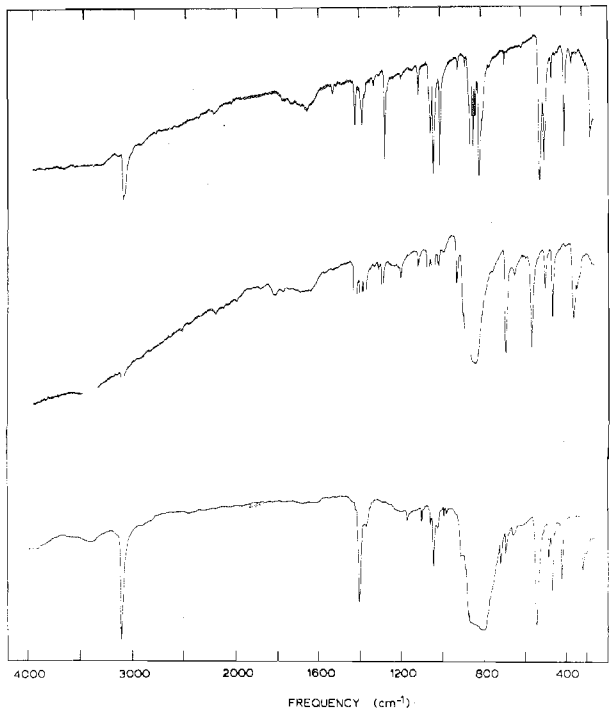

Figure 13. Infrared spectra of room-temperature KBr pellets of biferrocenylene (top), biferricenylenium$^+$PF$_6^-$ (middle), and biferricenylenium^{2+}(PF$_6^-$)$_2$ (bottom). The top abscissa is for the upper two spectra, while the bottom abscissa is for the lowest spectrum.

The large quadrupole splitting (2.86 mm/sec at 300°K) and negative field gradient of biferricenylenium(2+) (asymmetry parameter $\eta < 0.4$) have been discussed.[19] Recall that ferricenium ion has a small ΔE_Q. In short, the delocalization of e_{2g} electrons and the resultant loss of orbital angular momentum of these electrons leads to a large negative field gradient because the e_{2g} electrons with $\langle e_{2g}|\hat{H}_{QS}|e_{2g}\rangle = {}^4/_7\langle r^{-3}\rangle$ no longer contribute appreciably to the field gradient and the contribution from the a_{1g} electrons is *negative* with $\langle a_{1g}|\hat{H}_{QS}|a_{1g}\rangle = -{}^4/_7\langle r^{-3}\rangle$. The marked reduction in $\langle e_{2g}|\hat{H}_{QS}|e_{2g}\rangle$ is to be expected because the operator $\hat{H}_{QS}$ transforms as l^2, where $\hat{l}$ is the orbital angular momentum operator. As we have seen, the orbital angular momentum of the single unpaired e_{2g} electron in biferricenylenium(1+) appears to be quenched.

The question whether the interaction between the two Fe(III) centers in biferricenylenium(2+) is the result of direct exchange or superexchange still remains. In the next section we will present evidence favoring a direct-exchange interaction, but not before the infrared spectroscopy of biferricenylenium(n+) (n = 0, 1, 2) is considered.

The ir spectra of biferrocenylene and biferricenylenium(n+) (n = 1, 2) are shown in Figure 13 and summarized in Table IX. Biferrocenylene, unlike ferrocene or biferrocene, shows four strong features in the low-energy region. It is tempting

Table IX. Infrared Data for Biferrocenylene Systems

Biferrocenylene	Biferricenylenium$^{+}PF_6^{-}$	Biferricenylenium$^{+}I_5^{-}$	Biferricenylenium$^{2+}(PF_6^{-})_2$
257 ms			
347 w	310 mw	309 w	291 vw
384 s	323 m	330 sh	308 mw
447 w	338 ms	340 s	325 m
483 s	443 ms	441 s	425 m
			472 ms
505 s	480 m	478 m	488 mw
	546 s (PF_6^{-})		543 vs (PF_6^{-})
679 w	631 w	610 w	648 sh
	674 s	673 ms	658 w
781 sh			695 mw
			721 mw
804 s			
824 m	750 | 900 } vs multiplet (PF_6^{-})	824 s	750 | 900 } vs multiplet (PF_6^{-})
837 ms			
850 ms		846 w	
875 w			
911 w	917 m		914 m
			983 w
1001 s	1007 mw		996 w
1031 s	1035 ms	1040 ms	1028 mw
1046 m	1054 mw	1055 sh	1045 ms
	1061 mw		1061 mw
1105 mw	1107 w	1105 w	1104 w
1191 vw	1192 w		1173 w
1271 s	1282 m	1275 mw	
	1299 vw		
1325 w	1321 vw	1316 w	
1345 vw	1343 vw		
1372 mw	1363 m		1371 mw
	1371 ms	1370 mw	
1384 m			
1390 sh	1390 ms	1386 m	
1401 w	1405 sh	1408 sh	1402 s
1420 m	1419 s	1416 m	
1600 | 1800 } w multiplet	1600 | 1850 } w multiplet		
2217 vw	2207 vw		
3100 ms multiplet	3124 w	3100 m multiplet	3103 s

to assign these to the symmetric ring–metal–ring stretch (257 cm^{-1} (ms)), the symmetric ring–metal–ring tilt (384 cm^{-1} (s)), the asymmetric ring–metal–ring stretch (483 cm^{-1} (s)), and the asymmetric ring–metal–ring tilt (505 cm^{-1} (s)) by analogy with ferrocene. The symmetric modes have become ir active due to the lower molecular symmetry for biferrocenylene. The only difference in the *low-energy* region between mono- and dioxidized biferrocenylene is the appearance of a strong feature at 472 cm^{-1} for the dioxidized form. Other discernible differences between the ir spectra of the mono- and dioxidized forms are the absence of bands in the 1200–1300-cm^{-1} region and weaker bands in the 1600–1800-cm^{-1} region of the dioxidized compound. This is reminiscent of what happens when one oxidizes ferrocene to ferricenium(1+) ion; there is a dramatic decrease in intense bands in the ferricenium spectrum relative to the ferrocene spectrum.[35] Thus, in certain regions of the ir spectrum of biferricenylenium(1+) there appear to be bands associated with a ferrocene-type molecule. These bands occur in approximately the same place as found for biferrocenylene. If distinct bands are seen for the Fe(II) and Fe(III) centers in the biferricenylenium(1+) spectrum, this would imply a thermal electron-transfer rate *less* than $\sim 10^{13}$ sec^{-1}. This contradicts the photoelectron work and additional work is needed to clarify this. In passing, the very interesting biferricenylenium(1+) band at 674 cm^{-1} is to be noted.

[1.1]Ferrocenophane Systems. ^{57}Fe Mössbauer spectroscopy has shown that on the Mössbauer time scale the I_3^{-} salt of cation IVb is of the mixed-valence type at room temperature (electron-transfer rate $< 10^7$ sec^{-1}) while the $I_3^{-}\cdot 0.5I_2$ salt of cation IVa gives a spectrum that can be interpreted as a superposition of signals from both mixed- and average-valence species.[18] In both cases lowering the temperature of the sample led to an increase in the average-valence species and we tentatively associated the change in spectra with a phase transition wherein the Fe–Fe distance is changed to permit greater Fe–Fe exchange interaction. A puzzling feature was found in the least-squares fitting of the 4.2°K spectra. The areas of the two doublets supposedly arising from the mixed-valence species were not equal. We have collected and herewith report additional data on these interesting systems.

In an effort to understand better the temperature dependence of the Mössbauer spectra as noted above a new sample of 1,12-dimethyl[1.1]ferricenophanium$^{+}I_3^{-}$ was prepared, and, as Figure 14 shows, ^{57}Fe Mössbauer data were collected at six different temperatures from 300 to 4.2°K. At the outset it should be noted that the 300 and 4.2°K spectra are essentially superimposable with the 300 and 4.2°K spectra we reported. Added insight is obtained, for, as Figure 14 shows, as the temperature is lowered to 80°K, the inner doublet contracts and broadens gradually, whereas, below 80°K the relative intensity of the inner feature increases. The inner "doublet", of course, arises from a paramagnetic ferricenium site. The behavior seen is perhaps typical of paramagnetic relaxation in a Mössbauer spectrum wherein the relaxation appears to be almost "frozen" in the 4.2°K spectrum. As can be seen in Figure 14 and Table X the inner absorption in the 4.2°K spectrum can be fit to the three features expected for a spin $^1/_2$ coupling to the ^{57}Fe nucleus. Contrary to our earlier reporting, it appears that the "average-valence" shoulders with $\Delta E_Q = 1.84$ mm/sec do *not* appear to change appreciably with respect to relative area as the temperature is decreased (the slight temperature dependence could be due to differences in

Table X. Mössbauer Parameters for [1.1]Ferrocenophane Systems

Compd	T, °K	ΔE_Q, mm/sec	δ,[a] mm/sec	Γ,[b] mm/sec	Rel areas[c]
[1.1]Ferricenophanium$^+I_3^-\cdot 0.5I_2$	300	2.204 (16)	+0.422 (16)	0.430 (9), 0.436 (11)	1.00
		1.763 (16)	+0.451 (15)	0.142 (11), 0.182 (15)	0.22
		0.182 (8)	+0.418 (8)	0.307 (7), 0.273 (7)	1.00
	4.2	2.362 (21)	+0.528 (21)	0.280 (15), 0.280 (15)	0.28
		1.839 (6)	+0.532 (6)	0.278 (5), 0.283 (5)	1.00
		0.201 (8)	+0.531 (8)	0.387 (10), 0.316 (7)	0.79
1,12-Dimethyl[1.1]ferricenophanium$^+I_3$	300	2.375 (5)	+0.449 (5)	0.303 (4), 0.300 (5)	1.00
		1.855 (813)	+0.427 (813)	0.552 (417), 1.536 (882)	~0.05
		0.613 (20)	+0.417 (20)	0.575 (27), 0.385 (9)	1.00
	190	2.408 (8)	+0.495 (8)	0.301 (6), 0.310 (6)	0.94
		1.887 (55)	+0.502 (55)	0.342 (46), 0.339 (46)	0.18
		0.176 (31)	+0.473 (31)	0.725 (43), 0.489 (11)	1.00
	140	2.407 (5)	+0.514 (5)	0.298 (4), 0.305 (4)	0.90
		1.849 (21)	+0.528 (21)	0.195 (18), 0.241 (23)	0.10
		0.241 (32)	+0.451 (32)	1.266 (103), 0.564 (10)	1.00
	100	2.424 (6)	+0.525 (6)	0.250 (10), 0.256 (10)	0.63
		2.159 (54)	+0.533 (54)	0.713 (30), 0.731 (33)	1.00
		0.184 (86)	+0.516 (86)	0.804 (103), 0.606 (31)	0.61
	80	2.436 (3)	+0.526 (3)	0.206 (4), 0.210 (4)	1.00
		2.201 (18)	+0.530 (18)	0.679 (12), 0.694 (13)	0.21
		0.256 (19)	+0.523 (19)	0.725 (30), 0.534 (13)	0.11
	4.2	2.425 (3)	+0.541 (3)	0.255 (3), 0.274 (3)	0.89
		1.928 (23)	+0.554 (23)	0.415 (18), 0.469 (18)	0.40
			+0.331 (12)	0.588 (20)	0.42
			+0.654 (291)	0.588 (20)	0.22
			+0.401 (62)	0.588 (20)	1.00
1,12-Dimethyl[1.1]ferricenophanium$^{2+}(DDQH^-)_2$	300	2.168 (3)	+0.430 (3)	0.421 (4), 0.389 (3)	
	4.2	2.183 (8)	+0.522 (8)	0.429 (9), 0.420 (9)	

[a] Relative to iron foil; the standard deviations are given in parentheses. The absolute error in the above measurements is ~0.2%. [b] Full width at half-height taken from the lorentzian fitting program. Lines are listed with those at more negative velocities first. [c] Ratio of the area of a quadrupole doublet to the largest quadrupole doublet area in the spectrum. In every case both lines in a quadrupole doublet have the same area.

recoilless fraction). It is still our contention that the configurational flexibility of cation IVb coupled with the packing with the I_3^- counterions leads to the presence of both mixed- and average-valence (with respect to Mössbauer time scale) species. Our expectations as to the flexibility of cation IVb grow, in part, from the X-ray structure[41] of the unoxidized 1,12-dimethyl[1.1]ferrocenophane which shows two crystallographically distinct molecules with two different Fe–Fe distances [4.620 (2) and 4.595 (2) Å].

The variable-temperature magnetic susceptibility data for 1,12-dimethyl[1.1]ferricenophanium$^+I_3^-$ and [1.1]ferricenophanium$^+I_3^-\cdot 0.5I_2$ are illustrated in Figure 15 and are summarized in Table XI. The data for the latter compound are quite similar to those for ferricenium triiodide and, upon fitting to the theoretical equations, yield the parameters δ = 300 cm^{-1}, $\Delta > 900$ cm^{-1}, $\epsilon = 50$ cm^{-1}, and $k' = 0.80$ which are not unlike those for $[Fe(cp)_2]I_3$. No EPR signal could be obtained for the $I_3^-\cdot 0.5I_2$ salt of cation IVa for either glasses at 77°K or for the pure solid at 12°K. This is characteristic of a ferricenium system that is not very distorted.

The EPR spectral characteristics for the I_3^- salt of cation IVb are quite unusual because of the large g anisotropy. Fitting the g values and susceptibility data for this compound to the ligand field model presented in the Appendix gives the parameters summarized in Table IV. The value of g_y is not fit well. As in the biferricenylenium(1+) and 1',6'-diiodobiferricenium(1+) cases, the fit requires the $^2A_{1g}$ excited state to move close to and become highly mixed with the ground state. This is reflected in the lower magnetic moment of this compound as compared to [1.1]ferricenophanium$^+I_3^-\cdot 0.5I_2$ and in the ease of detection of an ESR signal. All in all, however, the agreement between experiment and theory is not as good for this system as it is for the others. The excellent analysis and crystallinity of the 1,12-dimethyl[1.1]ferricenophanium$^+I_3^-$ sample and the similarity of EPR spectra for 1,2-dimethyl[1.1]ferricenophanium(1+) doped into the dioxidized $DDQH^-$ compound seemingly eliminate an explanation of the reported EPR features as being due to an impurity.

Table XI. Variable-Temperature Magnetic Susceptibility Data for [1.1]Ferricenophanium Systems: (A) [1.1]Ferricenophanium$^+I_3^-\cdot 0.5I_2$, (B) 1,12-Dimethyl[1.1]ferricenophanium$^+I_3^-$, (C) 1,12-Dimethyl[1.1]ferricenophanium$^{2+}(DDQH^-)_2$

$10^3\chi_M^{cor}$,[a] cgsu/mol			
A	B[b]	C[c]	T, °K
3.14			290
3.46		0.40	255
3.72		0.46	221
4.11		0.51	191
4.62		0.58	160
5.54		0.71	121
8.33			80
10.3	7.64	1.30	58
12.8	9.89	1.43	46.5
20.0	17.6	2.88	28.4
48.5	26.1		19.2
			13.0
71.7	57.1		8.2
	93.3	11.6	5.4
100.4	129.6		4.2

[a] Molar paramagnetic susceptibilities are corrected for background and for diamagnetism of the compound. Compound diamagnetism is from Pascal's constants and the values are (A) -457.8×10^{-6} cgsu, (B) -425.2×10^{-6} cgsu, and (C) -502.5×10^{-6} cgsu. [b] μ_{eff}(av) = 1.98 BM. [c] μ_{eff}(av) = 0.75 BM.

The most interesting and enlightening result from this study is that the dioxidized 1,12-dimethyl[1.1]ferricenophanium^{2+}-$(DDQH^-)_2$ is *diamagnetic* in the range 4.2–300°K. As can be seen in Table XI this compound shows, analogous to the $DDQH^-$ salt of biferricenylenium(1+), a small residual paramagnetism with a temperature-independent μ_{eff} of 0.75 BM. Unfortunately, 1,12-dimethyl[1.1]ferrocenophane decomposes in concentrated sulfuric acid, and as such we were not able to prepare other dioxidized salts (see the Experimental Section for additional comments).

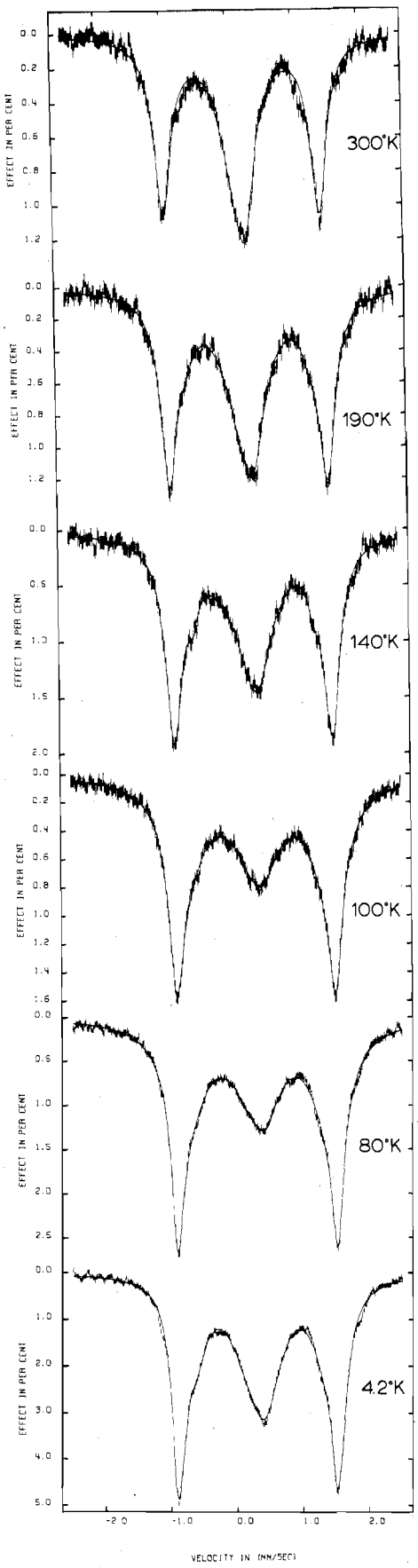

Figure 14. Iron-57 Mössbauer spectra of 1,12-dimethyl[1.1]-ferricenophanium$^+I_3^-$ at various temperatures. The velocity scale is referenced to the Co in Cu source.

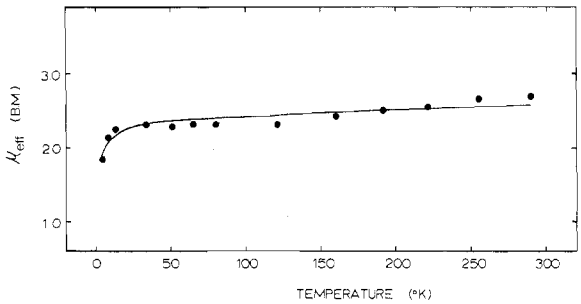

Figure 15. Effective magnetic moment (μ_{eff}) vs. temperature curve for [1.1]ferricenophanium$^+I_3^-\cdot 0.5I_2$. The line is a theoretical fit to the equations in the Appendix.

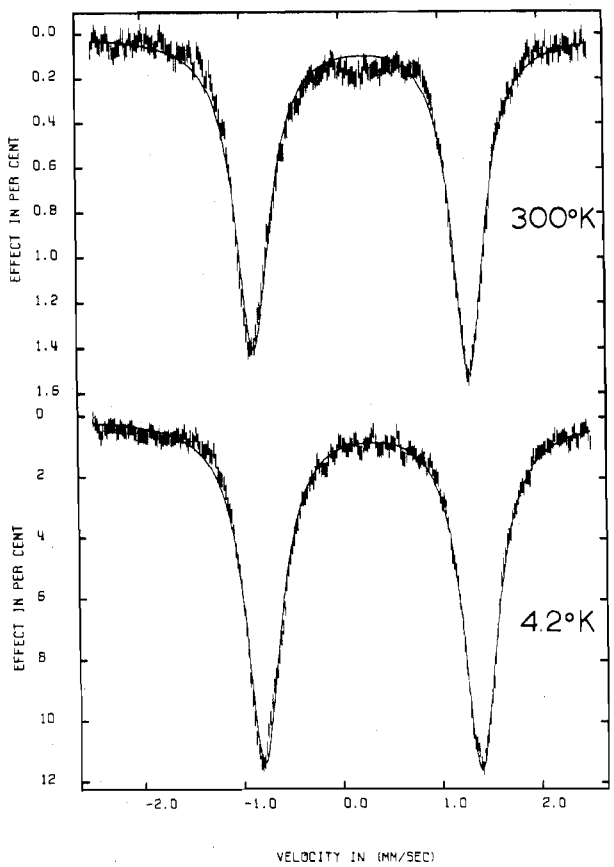

Figure 16. Iron-57 Mössbauer spectra of 1,12-dimethyl[1.1]-ferricenophanium^{2+}(DDQH$^-$)$_2$ at 300 and 4.2°K. The velocity scale is referenced to the Co in Cu source.

The ^{57}Fe Mössbauer data on this DDQH$^-$ salt of cation IVb provide additional insight into the electronic structure of cation IVb, $n = 2$. The 300 and 4.2°K spectra (see Figure 16) each show one quadrupole-split doublet with $\Delta E_Q = \sim 2.17$ mm/sec, which is to be compared with biferricenylenium(2+) where $\Delta E_Q = \sim 2.9$ mm/sec (see Tables II and X). The magnetically perturbed (26-kG longitudinal field) Mössbauer spectrum of the DDQH$^-$ salt of cation IVb, $n = 2$, is shown in Figure 17. In contrast to biferricenylenium(2+), η is quite large for this system with a value of ~ 0.8, and the sign of the field gradient appears to be positive (with large η two directions are almost equivalent with respect to the field gradient, and its sign becomes difficult to determine). The large value of η indicates that the ferricenium centers in this molecule are very distorted from axial symmetry.

The diamagnetism of and Mössbauer results for cation IVb, $n = 2$, can be taken to indicate that there is an appreciable distortion as a result of the iron atoms having moved to establish a direct Fe–Fe electron-exchange interaction where the

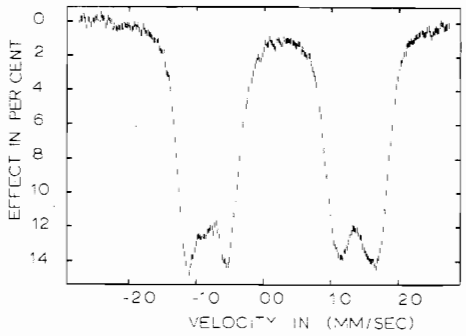

Figure 17. Magnetically perturbed (27-kG longitudinal field) ^{57}Fe Mössbauer spectrum of 1,12-dimethyl[1.1]ferricenophanium^{2+}-$(DDQH^-)_2$ at 4.2°K. The velocity scale is referenced to the Co in Cu source.

triplet state of the molecule lies in excess of ~400 cm^{-1} above the ground singlet. It does not seem at all reasonable that a superexchange interaction propagated by the two methylene bridges would be viable enough to give $J >$ ~400 cm^{-1}. At this time it is our conclusion that cation IVb, $n = 2$, owes its diamagnetism to a direct Fe–Fe exchange interaction *and* that this strongly implicates direct exchange-type interactions in the other systems.

In all the systems which show evidence for exchange (i.e., 1',6'-diiodobiferricenium(1+), biferricenylenium(1+), and 1,12-dimethyl[1.1]ferricenophanium(1+)), the ligand field parameters indicate that the $^2A_{1g}$ state has moved close in energy to the ground state, the lower energy E'' Kramers doublet from the $^2E_{2g}$ state. This observation is important because it seemingly reflects the greater electron-transfer rate in these systems. Since the ligand field theory as presented in the Appendix is not treating these cations as two metal centers, the movement of the $^2A_{1g}$ state could be an artifact of the ligand field model. The rapid exchange of the "hole" (electrons) between the two metal sites would be expected to quench the orbital agular momentum of the "hole" (electrons) involved in the exchange. That is, ferrocene and ferricenium orbitals are mixed in the delocalized ground state of these cations and the admixture gives a more magnetically isotropic species.

Electronic spectral data for the various [1.1]ferrocenophane species are collected in Table XII. The most interesting feature is the band for cation IVa, $n = 1$ at 13,300 cm^{-1} (ϵ 3350). Cation IVb, $n = 1$ does *not* have such a band and perhaps this relatively intense 13,300 cm^{-1} band is the intervalence (IT) band for cation IVa, $n = 1$.

Comments on the "Intervalence-Transfer" Band. In the electronic absorption spectra of biferricenium(1+), 1',6'-diiodobiferricenium(1+), and biferricenylenium(1+) there are bands in the near-ir region which are not present in the analogous $Fe^{II}Fe^{II}$ and $Fe^{III}Fe^{III}$ molecules. These band systems arise from electronic transitions as indicated in Figure 9; in the localized mixed-valence case of biferricenium(1+) the band can be called an "intervalence-transfer" band. Of course, in the situation where the interaction between the two Fe centers is large we approach the case where there is a very small barrier in the ground state, and in effect the ground state is completely delocalized with respect to the two iron centers. In this limit the one unpaired electron in the case of a direct Fe–Fe exchange is in an Fe–Fe bonding orbital and the near-ir electronic band results from a transition of this electron to the Fe–Fe antibonding orbital. We believe that an evaluation of the thermal intervalence-transfer rates from the equations of Hush coupled with the characteristics of the near-ir bands for the above molecules is suspect for the following three reasons. (1) The extent of interaction or noncrossing (H_{res} in Figure 9) needs to be gauged to evaluate E_{th}; this is not treated with

Table XII. Electronic Absorption Data for [1.1]Ferrocenophane Systems at Room Temperature

Compd	$h\nu_{max}$, nm	$h\nu_{max}$, cm^{-1}	ϵ, M^{-1} cm^{-1}	$\Delta E_{1/2}$,[d] cm^{-1}
[1.1]Ferrocenophane[a]	438	22,800	180	
	320	31,300 sh	245	
1,12-Dimethyl[1.1]-ferrocenophane[a]	440	22,700	205	
	320	31,300	210	
1,12-Dimethyl[1.1]-ferrocenophane[b]	441	22,700	220	
	320	31,300 sh	250	
	282	35,500 sh	~2,400	
	250	40,000 sh	6,840	
	<210	>48,000		
[1.1]Ferricenophanium$^+$-$I_3^-\cdot 0.5I_2$[b]	750	13,300	3,350	3080
	361[c]	27,700	25,800	
	291[c]	34,400	50,200	
	245	40,800	15,100	
	<210	>48,000		
1,12-Dimethyl[1.1]-ferricenophanium$^+I_3^-$[b]	809	12,400 sh		
	785	12,700	651	3300
	680	14,700	578	
	630	15,900 sh		
	550	18,200 sh		
	360[c]	27,800	12,800	
	290[c]	34,500	27,100	
	247	40,500	21,500	
	<210	>48,000		

[a] Ethanol solution. [b] Acetonitrile solution. [c] These bands are due to absorptions by I_3^- as per A. I. Popov and R. F. Swensen, *J. Am. Chem. Soc.*, 77, 3724 (1955). [d] Half-width estimated at the point where $I_\nu \nu_{max}/I_{max}\nu = 1/2$.

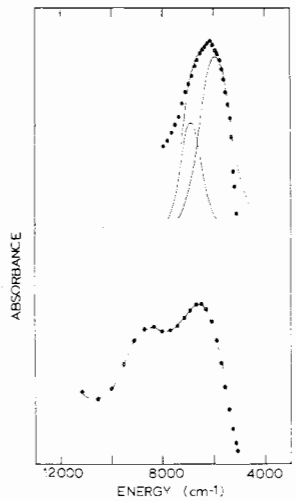

Figure 18. The 77°K absorption spectra of biferricenium$^+PF_6^-$ (top) and biferricenylenium$^+I_5^-$ (bottom) in the near-ir region (KBr pellets); a suggested resolution of the top spectrum into two gaussian bands is given, whereas the lower spectrum clearly shows two bands.

the simple Hush equation[4] where $E_{th} = E_{op}/4$. For two paramagnetic ions the degree of interaction can be approximated by the exchange parameter in the normal isotropic exchange Hamiltonian, $\hat{H} = -2J\hat{S}_1\cdot\hat{S}_2$. (2) The near-ir band for biferricenylenium(1+) is shouldered at room temperature and is clearly resolved into two bands at low temperatures, as can be seen in Figure 18. This has been noted before[17] and has been attributed to the presence of yet another low-lying excited state, the $^2A_{1g}$ ferricenium "hole" state where the "hole" is in the a_{1g} orbital. In short, the electronic structure is more complicated than is represented in Figure 9 and would require a more complex theory to determine E_{th}. (3) In view of the recently[35] exposed complexity of the vibronic characteristics for various ferricenium ions, it seems likely that the diagram is oversimplified in the sense that it assumes only one configuration coordinate for *both* the optical and thermal

processes and it assumes that the electronic states are nondegenerate.[42] Thus, the near-ir bands of biferricenium(1+) and 1',6'-diiodobiferricenium(1+) are very similar with respect to both position and width; however, the thermal electron-transfer rates are clearly quite different. Finally, the very recent results[20] on singly oxidized diferrocenylacetylene should be noted. An "intervalence-transfer" transition was observed in the near-infrared region and it was concluded "that the intervalence electron transfer can occur exclusively through the ligand system, inasmuch as the iron–iron distance (estimated to be 6.5 Å in a cis conformation and 7.3 Å in a trans) is too large to involve direct metal–metal overlap". It would only be too interesting to know the *thermal* electron transfer rate for singly oxidized diferrocenylacetylene.

Experimental Section

Compound Preparation. Samples of biferrocene,[43] biferrocenylene,[44,45] and 1,12-dimethyl[1.1]ferrocenophane[46] were all prepared according to literature methods. Analytical data from the University of Illinois School of Chemical Sciences microanalytical laboratory are given in Table I. Our initial sample of 1,12-dimethyl[1.1]-ferrocenophane and a sample of [1.1]ferrocenophane were gifts generously supplied by Professor W. E. Watts. An additional sample of the former was prepared by us and great difficulty was encountered in the preparation of the precursor 1,1'-bis(α-cyclopentadienylideneethyl)ferrocene according to the method of Watts[46] (ten unsuccessful attempts, five times exactly according to directions and five with variations in amounts of reactants, solvent, time of reaction, and temperature). In our hands the first attempt using another literature method[47] provided a quantitative yield of the material. Since this preparation occurs in the literature only in Czechoslovakian, an annotated translation will be given here.

To a 1000-ml flask equipped with a stirrer were added 500 ml of absolute ethanol, 22 g (0.085 mol) of 1,1'-diacetylferrocene, 22.4 g (0.34 mol) of freshly distilled cyclopentadiene, and 90 g of NaOH dissolved in 100 ml of degassed water. All operations were performed under a nitrogen atmosphere. The reaction mixture was stirred for 4 hr at room temperature (at the beginning the temperature rose to 40°). Just after 1.5 hr a dark red crystalline compound began to separate, accompanied by dissolution of the originally incompletely dissolved ferrocene. After stirring was completed, the reaction mixture was allowed to stand overnight at room temperature. The crystalline precipitate was filtered and washed with a little absolute ethanol. The reported yield was 93.5%, but we obtained a quantitative yield. The compound can be recrystallized from 65% ethanol–water. The reported melting point is 134°; however, our compound consistently melted at a lower temperature (110°) to give a tarlike material. The proton NMR spectrum and chemical analysis (see Table I) confirmed that it was the correct compound.

A sample of 1',6'-diiodobiferrocene[48] was prepared as reported and was characterized by mass spectrometry and melting point (166°; lit. mp 168°).

The iodine oxidation compounds were all prepared in the same fashion. The parent ferrocene was dissolved in benzene, and a stoichiometric amount of iodine dissolved in benzene was added dropwise with rapid stirring. The resulting solid was filtered, washed with a little benzene, and vacuum dried. See Table I for analyses. As can be seen from the table, biferrocenylene comes down as an I_2^- salt, and if this material is recrystallized from acetonitrile with excess iodine, black needles of the I_5^- salt form. This was repeated several times, and the analytical results indicate a consistent product composition. Crystals can be grown from acetone for most of the iodides; however, there is some decomposition.

Trichloroacetate salts were prepared by dissolving stoichiometric amounts of the parent ferrocene and trichloroacetic acid in benzene. The solution was bubbled with oxygen for ~15 min and then was allowed to stand at room temperature, whereupon crystals slowly formed. These were filtered, washed with benzene, and dried. Analytical data are in Table I.

The $DDQH^-$ salts were prepared with 2,3-dichloro-5,6-dicyanobenzoquinone according to Brandon and others[49] and the analytical data are given in Table I. The anion was found to be $DDQH^-$, not the radical DDQ^-; see our previous paper.[16]

The PF_6^- salts were prepared by dissolving the parent ferrocene (~100 mg) in ~1 ml of concentrated H_2SO_4. The solution was allowed to stand at room temperature for ~15 min; then it was cooled in ice and slowly diluted to a volume of ~10 ml with cold water. The cold solution was filtered and the filtrate was added to a concentrated aqueous solution of NH_4PF_6. The solid that formed was filtered and washed with H_2O and dried in vacuo over P_2O_5 for at least 24 hr. The PF_6^- salts can be recrystallized from warm water with a little acetone added.

Biferricenylenium$^+PF_6^-$ was prepared from the dioxidized compound (in many preparations the dioxidized compound contained small amounts of the monooxidized compound) by dissolving it in pH 7 water (formed a red solution). The dark green monooxidized biferricenylenium$^+PF_6^-$ slowly precipitated as platelike crystals.

The stability of α-ferrocenyl cations is beyond question.[50] These cations are readily formed in concentrated sulfuric acid. It is, thus, not surprising that 1,12-dimethyl[1.1]ferrocenophane decomposes when oxidized in this medium. The first step is probably the protonation of the iron atoms. When the supposedly dioxidized PF_6^- salt is made as above, the EPR spectrum shows an isotropic, strong signal (g = 2.015 with a width of ~320 G) at 77°K. The chemical analysis is not that much in error. Anal. Calcd for $C_{24}H_{24}Fe_2(PF_6)_2$: C, 40.37; H, 3.39; Fe, 15.64. Found: C, 42.09; H, 3.62; Fe, 15.95. However, reduction of the compound with $SnCl_2$ and extraction in ligroin showed that the compound had decomposed (tlc on alumina consisted of two or more bands). The magnetism of 1,12-dimethyl[1.1]-ferricenophanium$^{2+}(PF_6^-)_2$ showed a room-temperature moment of 2.41 BM per iron and the variable-temperature curve of μ_{eff} was similar to that of a simple ferricenium compound in contrast to the $(DDQH^-)_2$ salt which is diamagnetic.

Physical Methods. EPR spectra were recorded on a Varian E-9 spectrometer equipped with an Air Products Heli-tran cryogenic device which allowed sample temperatures as cold as ~12°K as per an iron-doped gold thermocouple. A Varian controller was used for the 77°K to room temperature runs. EPR spectra were also recorded on a Varian Q-band spectrometer employing an E-110 bridge and E266 cavity. Direct immersion of the cavity and sample in liquid nitrogen gave the 77°K setting.

Variable-temperature (4.2–290°K) magnetic susceptibilities were measured with a PAR Model 150A vibrating-sample magnetometer as per a previous paper.

Iron-57 Mössbauer measurements were made on a constant-velocity type instrument, which has been described previously.[51]

Low-temperature (~20°K) electronic absorption spectra were recorded on a Cary 14 spectrophotometer using a Cryogenics Technology, Inc., "Spectrim" closed-cycle refrigerator. Samples were prepared as either 13-mm KBr pellets or Nujol mulls.

Appendix

The ground state of the ferricenium ion is the $^2E_{2g}$ state from the $(e_{2g})^3(a_{1g})^2$ configuration; the ground state is split into two Kramers doublets [E'' and (A', A'') in the D_5' point group] by spin–orbit coupling.[31,34,35] Crystal fields of symmetry lower than D_5 with an effective Hamiltonian of H' mix E'' and (A', A'') and consequently affect the energy separation between E'' and (A', A''). By far the lowest lying excited state is the $^2A_{1g}$ (E' in D_5') state from the $(e_{2g})^4(a_{1g})^1$ configuration. Present indications are that the baricenters [$\Delta_1 = E(^2A_{1g}) - E(^2E_{2g})$] of the $^2E_{2g}$ and $^2A_{1g}$ states are within ~2000 cm^{-1}. Using the imaginary d-function notation of $d_{\pm 2} = (\pm 2)$, an appropriate sixfold degenerate basis set for the $^2E_{2g}$ and $^2A_{1g}$ states is

$$|\bar{2}00\text{-}2\text{-}2|,\ |2\bar{0}0\text{-}2\text{-}2|,\ |22\bar{0}\text{-}2\text{-}2|,\ |2\bar{2}0\text{-}2\text{-}2|,\ |22\bar{0}0\text{-}2|,\ |2\bar{2}0\bar{0}\text{-}2|$$

Low-symmetry crystal field mixing within this basis set can be gauged by $\delta = \langle d_2^{\pm}|H'|d_2^{\pm}\rangle$ and $\epsilon = \langle d_2|H'|d_0\rangle$, while the spin–orbit interaction constant for the $^2E_{2g}$ state is taken as $\xi = -k'\xi$ ($\xi_0 \equiv 450$ cm^{-1}).[34]

Interactions with the two lowest[36] energy $^2E_{1g}$ excited states were also taken into account with the addition of the parameters $\sigma = \langle d_2|H'|d_1\rangle$, $\Delta_2 = E(^2E_{1g}{}^a) - E(^2E_{2g})$ and $\Delta_3 = E(^2E_{1g}{}^b) - E(^2E_{2g})$. The $^2E_{1g}{}^a$ state comes from the $(e_{2g})^3(a_{1g})^1(e_{1g})^1$ configuration and the $^2E_{1g}{}^b$ state is the lowest energy $^2E_{1g}$ state from the $(e_{2g})^2(a_{1g})^2(e_{1g})^1$ configuration. The interactions with these two $^2E_{1g}$ excited states were not

found to be very important; however, in certain cases a fit to the data did seem to require something additional to the parameters for the $^2E_{2g}$ and $^2A_{1g}$ states. When the $^2E_{1g}$ states were used in the fitting, values of Δ_2 and Δ_3 were taken from the electronic spectra; for example, for biferricenylenium(1+) Δ_2 = 21,500 cm^{-1} and Δ_3 = 30,400 cm^{-1}.

The EPR and, in some cases, the variable-temperature magnetic susceptibility data for a given compound were fit using the simplex minimization computer program STEPT.[52] Thus, all of the above interactions plus the Zeeman interaction were included in three 14 × 14 matrices, one for each magnetic field orientation.[53] The three matrices are diagonalized at various magnetic field values, and for each field orientation the *g* value and susceptibility are evaluated at the desired magnetic field value. The minimization computer program systematically (parameters are given different priorities) varies the parameters to obtain minimum deviation between the calculated and experimental quantities. Unfortunately, the computer program does not calculate correlation errors between the various parameters. The text should be consulted to assess the significance of the various parameters given in Table IV. It should also be noted that we have *not* elected to take into account any possible effects of a (pseudo) Jahn–Teller distortion as has been indicated as necessary to explain the magnetic properties of cobaltocene and to be possibly of importance for the ferricenium ion.[54]

Registry No. Ferrocene, 102-54-5; ferricenium$^+I_3^-$, 1291-35-6; ferricenium$^+$DDQH$^-$, 39291-57-1; biferrocene, 1287-38-3; biferricenium$^+I_3^-$, 39470-17-2; biferricenium$^+$TCA$^-$·2TCAA, 56195-95-0; biferricenium^{2+}(DDQH$^-$)$_2$, 39291-60-6; 1',6'-diiodobiferricenium$^+I_3^-$, 56030-43-4; biferrocenylene, 11105-90-1; biferricenylenium$^+I_2^-$, 55937-71-8; biferricenylenium$^+I_3^-$·0.5I_2, 55937-76-3; biferricenylenium$^+I_5^-$, 55937-72-9; biferricenylenium$^+$-BF_4^-, 39333-81-8; biferricenylenium$^+$DDQH$^-$, 52732-80-6; biferricenylenium$^+PF_6^-$, 52732-79-3; biferricenylenium picrate, 39333-82-9; biferricenylenium$^+$TCA$^-$·2TCAA, 55937-74-1; biferricenylenium^{2+}(DDQH$^-$)$_2$, 39291-59-3; biferricenylenium^{2+}(PF_6^-)$_2$, 51472-07-2; biferricenylenium^{2+}(TCNQ$^-$)$_2$, 55886-27-6; [1.1]-ferrocenophane, 1294-39-9; [1.1]ferricenophanium$^+I_3^-$·0.5I_2, 52655-94-4; 1,12-dimethyl[1.1]ferrocenophane, 1294-42-4; 1,12-dimethyl[1.1]ferricenophanium$^+I_3^-$, 52391-13-6; 1,12-dimethyl-[1.1]ferricenophanium$^+$DDQH$^-$, 55937-75-2; 1,12-dimethyl[1.1]-ferricenophanium^{2+}(DDQH$^-$)$_2$, 55886-29-8; 1,1'-diacetylferrocene, 1273-94-5; cyclopentadiene, 542-92-7.

References and Notes

(1) Camille and Henry Dreyfus Fellow, 1972–1977.
(2) M. B. Robin and P. Day, *Adv. Inorg. Chem. Radiochem.*, **10**, 247 (1967).
(3) G. C. Allen and N. S. Hush, *Prog. Inorg. Chem.*, **8**, 357 (1967).
(4) N. S. Hush, *Prog. Inorg. Chem.*, **8**, 391 (1967).
(5) D. O. Cowan and F. Kaufman, *J. Am. Chem. Soc.*, **92**, 219 (1970).
(6) F. Kaufman and D. O. Cowan, *J. Am. Chem. Soc.*, **92**, 6198 (1970).
(7) D. O. Cowan, R. L. Collins, and F. Kaufman, *J. Phys. Chem.*, **75**, 2025 (1971).
(8) D. O. Cowan, G. A. Candela, and F. Kaufman, *J. Am. Chem. Soc.*, **93**, 3889 (1971).
(9) D. O. Cowan, G. Pasternak, and F. Kaufman, *Proc. Natl. Acad. Sci. U.S.A.*, **66**, 837 (1970).
(10) D. O. Cowan, J. Park, M. Barber, and P. Swift, *Chem. Commun.*, 1444 (1971).
(11) D. O. Cowan, C. LeVanda, J. Park, and F. Kaufman, *Acc. Chem. Res.*, **6**, 1 (1973).
(12) D. O. Cowan and C. LeVanda, *J. Am. Chem. Soc.*, **94**, 9271 (1972).
(13) D. O. Cowan, C. LeVanda, R. L. Collins, G. A. Candela, U. T. Mueller-Westerhoff, and P. Eilbracht, *J. Chem. Soc., Chem. Commun.*, 329 (1973).
(14) U. T. Mueller-Westerhoff and P. Eilbracht, *J. Am. Chem. Soc.*, **94**, 9272 (1972).
(15) U. T. Mueller-Westerhoff and P. Eilbracht, *Tetrahedron Lett.*, **21**, 1855 (1973).
(16) W. H. Morrison, Jr., S. Krogsrud, and D. N. Hendrickson, *Inorg. Chem.*, **12**, 1998 (1973).
(17) W. H. Morrison, Jr., and D. N. Hendrickson, *J. Chem. Phys.*, **59**, 380 (1973).
(18) W. H. Morrison, Jr., and D. N. Hendrickson, *Chem. Phys. Lett.*, **22**, 119 (1973).
(19) W. H. Morrison, Jr., and D. N. Hendrickson, *Inorg. Chem.*, **13**, 2279 (1974).
(20) C. LeVanda, D. O. Cowan, C. Leitch, and K. Bechgaard, *J. Am. Chem. Soc.*, **96**, 6788 (1974).
(21) D. O. Cowan, J. Park, C. U. Pittman, Jr., Y. Sasaki, T. K. Mukherjee, and N. A. Diamond, *J. Am. Chem. Soc.*, **94**, 5110 (1972).
(22) C. U. Pittman, Jr., and P. L. Grube, *J. Appl. Polym. Sci.*, **18**, 2269 (1974).
(23) C. U. Pittman, Jr., and B. Surynarayanan, *J. Am. Chem. Soc.*, **96**, 7916 (1974).
(24) C. U. Pittman, Jr., Y. Sasaki, and T. K. Mukherjee, *Chem. Lett.*, **4**, 383 (1975).
(25) V. P. Alekseev, R. A. Stukan, and A. A. Koridze, *Izv. Akad. Nauk SSSR, Ser. Khim.*, 132 (1973).
(26) D. M. Duggan, A. Schlueter, H. B. Gray, and D. N. Hendrickson, unpublished work.
(27) R. A. Stukan, S. P. Gubin, A. N. Nesmeyanov, V. I. Gol'danskii, and E. F. Makarov, *Teor. Eksp. Khim.*, **2**, 805 (1966); U. Zahn, P. Kienle, and H. Eicher, *Z. Phys.*, **166**, 220 (1962); G. K. Wertheim and R. L. Herber, *J. Chem. Phys.*, **38**, 2106 (1963); T. Birchall and I. Drummond, *Inorg. Chem.*, **10**, 399 (1971); R. L. Collins, *J. Chem. Phys.*, **42**, 1072 (1965).
(28) D. Lupu, D. Barb, G. Filoti, M. Morariu, and D. Larina, *J. Inorg. Nucl. Chem.*, **34**, 2803 (1972).
(29) V. I. Gol'danskii, V. P. Alekseev, R. H. Stukan, and K. I. Turta, *Dokl. Akad. Nauk SSSR*, **213**, 867 (1973).
(30) G. C. Allen, M. B. Wood, and J. M. Dyke, *J. Inorg. Nucl. Chem.*, **35**, 2311 (1973).
(31) D. N. Hendrickson, Y. S. Sohn, and H. B. Gray, *Inorg. Chem.*, **10**, 1559 (1971).
(32) S. E. Anderson and R. Rai, *Chem. Phys.*, **2**, 216 (1973).
(33) Y. S. Sohn, D. N. Hendrickson, and H. B. Gray, *J. Am. Chem. Soc.*, **93**, 3603 (1971).
(34) D. N. Hendrickson, Y. S. Sohn, D. M. Duggan, and H. B. Gray, *J. Chem. Phys.*, **58**, 4666 (1973).
(35) D. M. Duggan and D. N. Hendrickson, *Inorg. Chem.*, **14**, 955 (1975).
(36) R. Prins and A. Kortbeek, *J. Organomet. Chem.*, **33**, C33 (1971).
(37) A. Horsfield and A. Wassermann, *J. Chem. Soc. A*, 3202 (1970).
(38) A. Horsfield and A. Wassermann, *J. Chem. Soc. A*, 187 (1972).
(39) W. L. Jolly, *Coord. Chem. Rev.*, **13**, 47 (1974).
(40) M. R. Churchill and J. Wormald, *Inorg. Chem.*, **8**, 1970 (1969).
(41) J. S. McKechnie, B. Bersted, I. C. Paul, and W. E. Watts, *J. Organomet. Chem.*, **8**, P29 (1967); J. S. McKechnie, C. A. Maier, B. Bersted, and I. C. Paul, *J. Chem. Soc., Perkin Trans. 2*, **2**, 138 (1973).
(42) H. G. Drickamer, C. W. Frank, and C. P. Slichter, *Proc. Natl. Acad. Sci. U.S.A.*, **69**, 933 (1972).
(43) M. D. Rausch, *J. Org. Chem.*, **26**, 1802 (1961).
(44) F. L. Hedberg and H. Rosenberg, *J. Am. Chem. Soc.*, **91**, 1258 (1969).
(45) M. D. Rausch, R. F. Kovar, and C. S. Kraihanzel, *J. Am. Chem. Soc.*, **91**, 1259 (1969); M. D. Rausch, *J. Org. Chem.*, **28**, 3337 (1963).
(46) T. H. Barr, H. L. Lentzner, and W. E. Watts, *Tetrahedron*, **25**, 6001 (1969).
(47) M. Furdik, S. Toma, and J. Suchy, *Chem. Zvesti*, **15**, 547 (1961).
(48) R. F. Kovar, M. D. Rausch, and H. Rosenberg, *Organomet. Chem. Synth.*, **1**, 173 (1971).
(49) R. L. Brandon, J. H. Osiecki, and A. Ottenberg, *J. Org. Chem.*, **31**, 1214 (1966); M. Ichikawa, M. Soma, T. Onishi, and K. Tamaru *Trans. Faraday Soc.*, **63**, 2528 (1967); Y. Omote, T. Komatsu, R. Kobayshi, and N. Sygiyama, *Tetrahedron Lett.*, **93** (1972).
(50) W. M. Horspool, R. G. Sutherland, and B. J. Thomson, *Chem. Commun.*, 729 (1970); W. M. Horspool, P. Stanley, R. G. Sutherland, and B. J. Thomson, *J. Chem. Soc. C*, 1365 (1971).
(51) B. Münck, P. G. Debrunner, J. C. M. Tsibris, and I. C. Gunsalus, *Biochemistry*, **11**, 855 (1972).
(52) J. C. Chandler, Program 66, Quantum Chemistry Program Exchange, Indiana University, Bloomington, Ind.
(53) W. H. Morrison, Jr., Ph.D. Thesis, University of Illinois, 1974.
(54) J. H. Ammeter and J. D. Swalen, *J. Chem. Phys.*, **57**, 678 (1972); J. H. Ammeter and J. M. Brom, Jr., *Chem. Phys. Lett.*, **27**, 380 (1974).